The Zn-Pb deposits of Casario (Ligurian Alps, NW Italy): Late Palaeozoic sedimentary-exhalative bodies affected by the alpine metamorphism

UNIVERSITÀ DEGLI STUDI DI TORINO

The Zn-Pb deposits of Casario (Ligurian Alps, NW Italy): Late Palaeozoic sedimentary-exhalative bodies affected by the alpine metamorphism

Piergiorgio Rossetti[a]*, Silvio Ferrero[b]

[a] Dipartimento di Scienze Mineralogiche e Petrologiche
Università di Torino - via Valperga Caluso, 35
I-10125 Torino, Italy

[b] Dipartimento di Geoscienze
Università di Padova - via Giotto, 1
I-35137 Padova, Italy

*Corresponding author.
E-mail address: piergiorgio.rossetti@unito.it

Abstract

In the Ligurian Alps (South-Western Italian Alps), Zn-Pb deposits occur within late Palaeozoic meta-sedimentary units belonging to the Briançonnais Zone near Casario (Tanaro valley). Different types of sulphide-rich, lens-shaped mineralizations are recognized: sphalerite-galena massive sulphide bodies, pyrite-rich lenses and sulphide-rich quartz–carbonate-chloritoid granofels. Sulphide lenses and host rocks are affected by at least three ductile deformation phases and by a polyphase alpine metamorphism, whose climax conditions are estimated, based on P-T pseudosection calculations, at T = 300-325 °C and P = 0.55-0.60 GPa. In all the mineralized lenses the ore minerals are represented, in variable amount, by Fe-poor sphalerite, galena, pyrite and arsenopyrite (± tetrahedrite, chalcopyrite and pyrrhotite); the gangue consists of quartz, carbonate (siderite-magnesite ± rhodochrosite s.s.), Fe-chloritoid, muscovite-phengite and chlorite. The mineralizations are associated with chloritoid – carbonate micaschists displaying a finely bedded texture, with sharp between-bed compositional contrast, which suggests their exhalative origin.

In spite of the tectono-metamorphic overprint, some pre-metamorphic features of the hydrothermal system are still recognized, like relics of the hydrothermal feeding system, primary growth textures and sulphide-rich microbreccias. These massive sulphide lenses, which share many characters with the SEDEX deposits, testify to the occurrence of an exhalative event of Upper Carboniferous age previously unrecognized in the Ligurian Briançonnais Unit.

Keywords: **massive sulphide deposit – exhalite - primary growth texture - metamorphic evolution - Ligurian Briançonnais**

1. Introduction

Massive sulphide bodies occur, at a world scale, in different districts, spanning a time range between Archean to Tertiary; these deposits have been, and still are, a major source of Pb, Zn, Cu, Ag and Au. Due to the complexity of macro- to microscopic characters, their (syn- to epigenetic) origin has been for decades the object of a hard debate in the Literature [1 and references therein]. Based on a number of geologic, petrologic and geochemical evidences, the occurrence of important exhalative ore-forming processes is now generally accepted, also due to the discovery of present-day hydrothermal vents on the ocean floor and sediment-covered spreading centers [2, 3]. The studies performed on massive sulphides have shown that the deposits occur in different palaeogeographic and tectonic settings, with highly variable textural and geochemical features; they are the result of complex ore-forming processes and later modifications related to deformation and metamorphic overprint [1, 4, 5 and references therein].

In the Ligurian Alps (South-Western Italian Alps: Fig. 1), Zn-Pb deposits occur within late Palaeozoic meta-sedimentary units in the Casario area, near Garessio, in the Tanaro valley. Though locally mined in the past, these deposits have been completely forgotten, or at best briefly mentioned, often as “dykes” [7] in the scientific Literature. The new data reported in this paper prove a relationship between the Zn-Pb deposits and an important exhalative event, late Carboniferous in age; the effects of the tectono-metamorphic overprint on the exhalative bodies are also discussed.

2. Geological framework

The Ligurian Alps (Fig. 1) are the south westernmost segment of the Western Alps collisional belt. They are composed of two main tectonic units, the Briançonnais Zone and Piedmont Zone, belonging to distinct palaeogeographic Domains: the Briançonnais Domain (in this sector called Ligurian Briançonnais Domain), part of the Palaeo-European continent, and the Piedmont Domain (l.s.). The latter includes the Prepiedmont Domain, or Piedmont Domain s.s., representing the Palaeo-European continental margin, and the Piedmont-Ligurian Domain, corresponding to the adjacent oceanic basin [8, 9]. As the study area occurs within the Briançonnais Zone and the massive sulphides formation is strictly related with its pre-alpine evolution, the following sections are devoted to the pre-Triassic geology of the Ligurian Briançonnais Zone.

2.1. Ligurian Briançonnais Zone

The Briançonnais Zone is derived from thinned Palaeo-European continental crust, according to Stampfli [10] formerly in continuity with the Hercynian chains of Corsica/Sardinia and Iberian Peninsula. It records the pre-Alpine history of the European crust related mostly to the Variscan orogenic cycle (Devonian–Carboniferous) and the subsequent late Palaeozoic – Mesozoic sedimentary evolution [8, 11]. In the Ligurian Alps, the Briançonnais Zone is composed of a relatively chaotic stacking of tectonic units which were in origin in palaeogeographic continuity. Based on their palaeogeographic setting, three sectors (inner, middle and outer) are recognized, each of them being composed of a crystalline basement and a Permo-Carboniferous cover [12].

2.1.1. Pre-Carboniferous basement

The crystalline basement occurs as isolated units mostly devoid of their late Palaeozoic to Mesozoic cover. These “crystalline massifs” crop out as allochthonous masses tectonically overlying the Upper Palaeozoic schists; they are mainly composed of orthogneiss, paragneiss, micaschist, amphibolite, migmatite and more rarely eclogitic and granulitic rocks [13]. They suffered a complex pre-alpine, magmatic and metamorphic evolution: particularly, a first Caledonian metamorphic event, at relatively HP-HT conditions, was followed by a Lower Carboniferous event (Variscan Cycle) under amphibolite facies conditions [14, 15]. The alpine metamorphism only caused a faint re-crystallization, with an exception being the Bagnaschino Massif, which was equilibrated under blueschist facies conditions [16, 17].

2.1.2. Permo - Carboniferous cover

The Permo-Carboniferous cover, also called “tegumento” (from the Latin *tegumen* = shell) in the Italian Literature, comprises meta-sedimentary to volcanic (l.s.) units [8, 16] whose dating is mostly inferred from field relationships and correlations with other sectors of the belt, due to the almost complete absence of fossil records.

The sedimentary series, mainly of continental affinity, starts with coarse to fine grained quartz-feldspatic sediments (*Lisio Formation:* lower Westphalian – Namurian), followed by fluvio-lacustrine sediments interbedded with locally

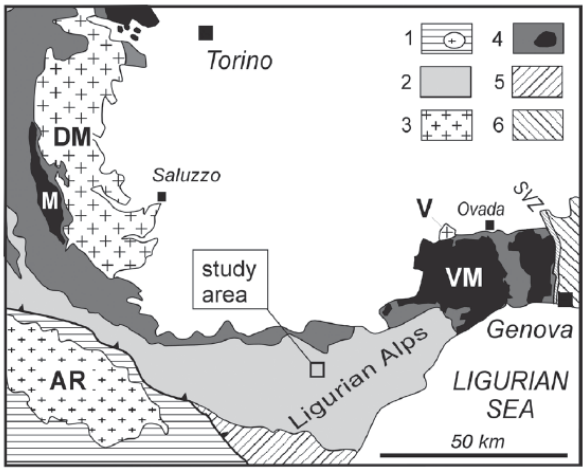

Fig. 1: Structural sketch map of the South-Western Alps. **1:** Helvetic Units and Argentera Massif (AR); **2:** Briançonnais Zone; **3:** Internal Crystalline Massifs (DM: Dora Maira, V: Valosio); **4:** Piedmont Zone, with main ophiolite bodies in black (VM: Voltri Massif, M: Monviso); **5:** Helminthoid Flysch nappe; **6:** Ligurian Nappes. SVZ: Sestri-Voltaggio Zone. Modified from [6].

fossiliferous graphitic lenses (*Ollano Formation*: upper Westphalian – Stephanian) and by fine grained, in part graphitic, metasediments, pertaining to different formations (*Viola Schists*, *Murialdo Formation* and *Gorra Schists*: Stephanian - Autunian?). The Palaeozoic series ends with medium- to coarse-grained clastic metasediments (*Briançonnais Verrucano*, of inferred Upper Permian age) related to erosion of the underlying ignimbrites.

Concerning the volcanic (l.s.) units, a first period of ignimbrites, tuffs, ashes and lavas of intermediate, mainly trachyandesitic composition for the Latest Carboniferous was followed, during the Early Permian, by a calc-alkaline series of pyroclastites, ashes, ignimbrites and rhyolites [18, 19, 11]. An early volcanic episode is given by ignimbritic rhyolite and pyroclastic agglomerate (*Case Lisetto metarhyolite*: Westphalian - Stephanian), cropping out within the Lisio and Ollano Formations [20]; the following episode is represented by andesitic lava and pyroclastite, transformed to metabasite (*Eze Formation*), interbedded within the Stephanian to Autunian sediments of the Viola, Murialdo and Gorra formations [19]. The third episode consists of ignimbrites connected to the final volcanic phase (*Melogno "porphyroids"*: Lower Permian). They occur in the inner and middle sectors, overlying the Carboniferous sediments, and crop out as huge bodies (mostly rhyolite to dacitic ignimbrite and pyroclastite) [21].

The Permo-Carboniferous cover has been affected by a low grade alpine metamorphism under blueschist to greenschist facies conditions [22], and records at least three ductile deformation phases [12; 9 and references therein].

During the Upper Carboniferous and Permian the Briançonnais Domain was characterized by the occurrence of structural highs and subsident trenches, the latters filled with hypabissal, effusive and pyroclastic materials mixed with continental sediments, related to an extensional geodynamic setting [8]. The lack of lateral continuity between many of the recognized units, which is a peculiar character of the Ligurian Briançonnais Zone, probably represents an inherited character, rather than the effect of the alpine deformation; the extensional setting probably also favoured the magma ascent [23 and references therein].

3. Geological framework of the Casario area

The study area ("Casario area" from a local place name) is located north-east of the Garessio village in the Chiapparo stream valley, which is a minor right-lateral valley of the Tanaro river (Fig. 2a). In this sector of the Ligurian Alps most of the tectonic units are represented by the lower Briançonnais units; particularly, the area is comprised within the southern portion of the "Pamparato – Murialdo Unit", which belongs to the inner Briançonnais domain tectonically overlying the external (i.e., more southerly) units. The Pamparato – Murialdo Unit overlies the Ormea Unit (and, east of the Tanaro river, the strongly similar Mallare Unit) and is, in turn, overlain by the Bagnaschino and the Piedmont Zone Units (Figs. 2a and 2b). A simplified cross-section showing the relationships between the main Units is shown in Fig. 2b.

3.1. The Pamparato – Murialdo Unit

The Pamparato – Murialdo Unit is composed of a pre-Namurian basement overlain by quartz-feldspatic metasediments (Lisio Formation); the upper part is represented by fine grained metasediments (Viola Schists, Murialdo Formation and Gorra Schists), with intercalations of meta-andesitic rocks (Eze Formation) [8]. Concerning the primary relationships between Viola Schists, Murialdo Formation and Gorra Schists, according to Cabella *et al.* [23, 24] the Viola Schists, of more internal palaeogeographic position, were interfingered with the more external Murialdo Formation and possibly with the lower part of the Gorra Schists; the upper part of the Gorra Schists would correspond to the top of the sequence.

An interpretative geological map of the area, based on 1:5000 mapping and strongly supported by the petrographic study, is shown in Fig. 3. In the same figure, Area 1 and 2 correspond to the main mineralized areas; a more detailed map of

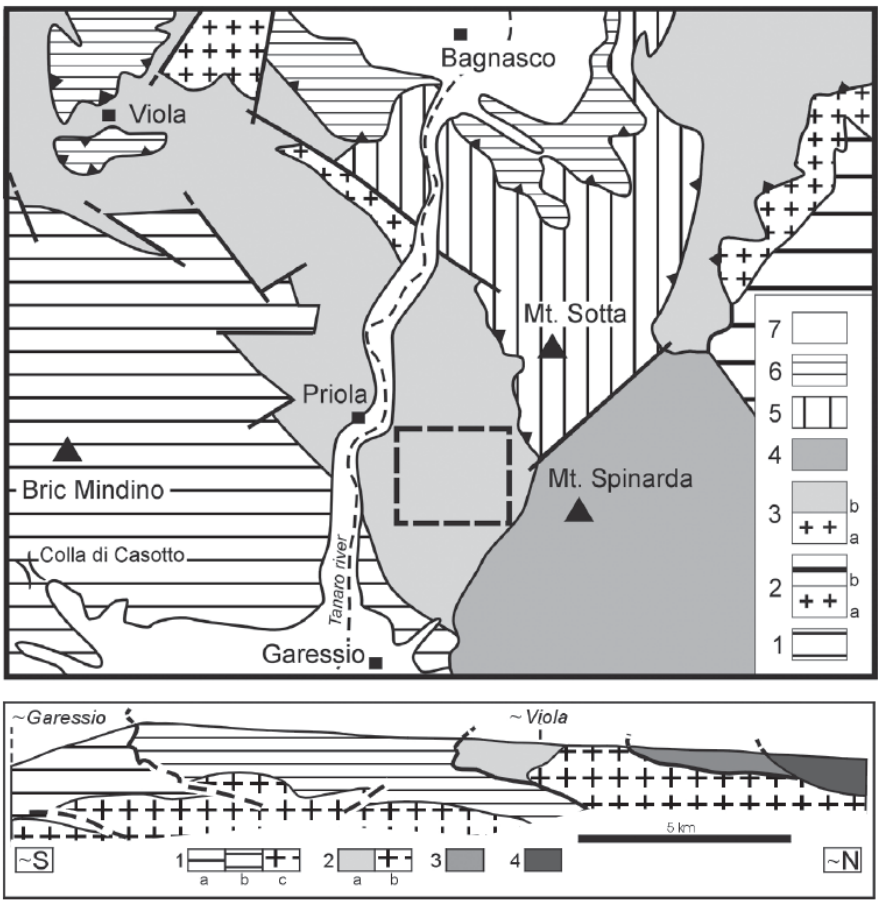

Fig. 2: a (above): Tectonic sketch-map of the Ligurian Alps in the study area. Briançonnais Zone:
1: Ormea unit (indifferentiated); **2, 3:** Mallare and Pamparato – Murialdo Units, respectively (a: crystalline basement, including the Lisio Formation; b: Permo-Carboniferous cover); **4:** Calizzano Massif (allochthonous basement unit). Piedmont Zone: **5:** Monte Sotta Unit (Meso-Triassic dolomite); **6:** indifferentiated Villanova (Permian-Scytic quartzite and Meso-Triassic carbonatic rocks) and Montenotte (of ophiolitic affinity) Units. **7:** undifferentiated tardo-orogenic Oligocene to Quaternary covers. The square shows the location of the Casario area. Simplified after [12]. **b** (below)**:** Strongly simplified sketch of the relationships between the tectonic units in the area along an idealized profile broadly oriented N-S (from the inner to the outer sector of the Ligurian Alps), west of Garessio. Ligurian Briançonnais Zone:
1: Ormea unit (a, b: Permo-Carboniferous cover, outer and inner sectors, respectively; c: crystalline basement); **2:** Pamparato – Murialdo Unit (a: Permo-Carboniferous cover; b: crystalline basement); **3:** Bagnaschino Unit. Piedmont Zone: **4:** Undifferentiated Monte Sotta – Villanova and Montaldo Units. Simplified after [12].

Area 1 is reported in Fig. 5. In the area two Formations crop out: the Murialdo Formation and the geometrically overlying Gorra Schists.

The *Murialdo Formation* only crops out along the lower part of the Chiapparo stream valley, over a thickness of about 200 m. It is composed of a monotonous sequence of metasedimentary rocks, mainly phyllites and fine grained dark micaschists; a typical feature of the formation is the occurrence of graphite, often abundant. Millimetre-thick milky quartz domains (possibly transposed quartz veins) occur interbedded in the micaschists. Close to the top of the Murialdo Formation, few small lenses of chloritoid – carbonate quartz-micaschists (not shown in Fig. 3) also crop out.

The overlying *Gorra Schists* are composed of a much more heterogeneous sequence, mainly consisting of very fine grained metasedimentary rocks, difficult to interpret in the field. For this reason, and because they contain the mineralized lenses, a petrographic study has been carried out (see below) and the rock-type terms used below are largely based on petrography.
Most of the formation is composed of fine grained carbonate ± chlorite micaschists, locally containing graphite concentrations ("Gorra Schists s.s." in Fig. 3). Interbedded in the Gorra Schists s.s., different types of schists, carbonatic rocks and sulphide lenses crop out, which are described in detail in Sections 4 and 5.
The contact with the underlying Murialdo Formation is mostly obscured by Quaternary cover. The occurrence of graphite enrichments also in the lower part of the Gorra Schists and the homogeneity of structural features in the two formations suggest, in agreement with Cabella *et al.* [23, 24], a stratigraphic character for the contact.

3.2. The massive sulphide deposits

The sulphide deposits always crop out within the Gorra Schists, along an at least 1500 m long, NNE-SSW trending band broadly parallel to the regional foliation (Fig. 3). This band is up to 100 metres thick and is located some tens of metres above the contact with the Murialdo Formation.

Few scattered data are available on the past mining and exploration activities in the area. Sulphide bodies are mentioned in a manuscript by Nicolis di Robilant (1786; in [25]), as tabular bodies of "*plomb luisant à grains fins contenant de l'argent*" (silver-bearing, fine grained "shining lead", i.e. galena), in the area between Priola and Garessio (Fig. 2a); during the XIXth century, the occurrence of ancient mines in the area is cited by different Authors [26, 27]. Between the last

decades of XIX century and the begin of XX century some underground mining occurred south of the Casario area, along the Valsorda creek (close to Garessio), where a sulphide mineralization was exploited following pre-existing galleries [28]. The old workings are now inaccessible, because flooded by water. During the XXth and at the beginning of the XXIst century several companies carried out some small scale exploration activities, in the Casario and nearby areas, confirming the occurrence of some high grade Zn-Pb (-Ag±Au) concentrations; some attempts to re-open the old mines were performed, but without success. At present, the only evidences of mining activities in the Casario area are given by remnants of old adits (mostly covered by landslides) and dumps; however, relatively good exposures occur along the creeks.

3.3. Structural framework

Both Formations are affected by at least three ductile deformation phases (F_1÷F_3); the main attitude of the foliation is broadly dipping 40° S [29].

F_1 is represented by isoclinal folds and associated axial plane foliation; apart from the hinges, the primary sedimentary surface S_0, which can be still recognized, mostly parallels the S_1 axial plane foliation, which broadly strikes E-W and dips steeply to moderately S (average dip 54°; Fig. 5 for Area 1).

The second deformation phase (F_2) is represented by folds ranging in geometry from open to tight, with a wavelength comprised between 1 and 5 m. F_2 axes are mostly sub-horizontal, E-W trending (Fig. 5); a S-verging, pervasive to spaced axial plane cleavage foliation S_2, mostly oriented 160/54 and crosscutting at low angle S_1, is associated with this deformation phase. Bigger folds show a Z geometry and verge S, as clearly seen along the contact between the Murialdo Formation and Gorra Schists (Fig. 3).

The third deformation phase (F_3) is represented by open cylindric folds with axes broadly dipping 10° towards SE. This deformation phase is less pervasive: in the carbonatic rocks ESE-trending open cylindric folds are observed, with joints above the hinges. Only locally, in the chloritoid-bearing phyllites a S_3 cleavage is observed in thin section. Massive sulphide lenses are clearly affected by all the deformation phases.

Brittle deformation structures are difficult to identify in the field, due to the amount of Quaternary cover; however, field mapping suggests that major displacements within the sequence do not occur. Small normal, subvertical faults oriented NNE-SSW showing centimetric displacement are locally observed, mostly in the northern area (Figs. 3 and 5). In the upper part of the Chiapparo stream (Figs. 3 and 5), some cataclastic horizons dipping 20-40° to the west are likely to represent minor thrust planes related to the emplacement of the overlying Monte Sotta nappe [29].

4. Petrography of the Gorra Schists

The sulphide mineralizations always occur within the Gorra Schists, in the two areas named Area 1 and Area 2 (Figs. 3 and 5). As already mentioned most of the formation is composed of fine grained *carbonate ± chlorite micaschists* ("Gorra Schists s.s.").

These rocks show under the microscope a banded structure, with interbedded, millimetre-thick quartz – carbonate ± albite and white mica ± chlorite ± graphite ± lawsonite domains along the S_1 foliation. Clastic quartz also occurs. The S_1 foliation is crosscut by S_2 crenulation planes where a second white mica generation forms, partly replaced by chlorite; only within the mica-rich domains a S_3 cleavage is observed. The carbonate abundance is highly variable; apatite, tourmaline, zircon and rutile are accessory.

Interlayered in the Gorra Schists s.s., the following rock-types occur as small outcrops:

Albite-micaschists, cropping out in the upper part of the sequence near Rionda Pass (Fig. 3) as up to few metres thick, some metres long lenses, light green in colour. Under the microscope these rocks display a well spaced, planar to anastomosed scistosity with alterned, sub-millimetre thick quartz – albite and white mica – rich domains. In the quartz - albite domains two plagioclase generations occur: a first one is represented by deeply sericitized, up to one millimetre-sized porphyroclasts; a second one by syn- to post-kynematic poikiloblastic albite. Porphyroclasts with fresh albite at rim are common. White mica occurs as coarse grained lamellae, unoriented or aligned along the S_1 foliation, partially transformed to chlorite; the quartz/albite ratio is variable. Clastic apatite is a typical accessory phase. Locally the albite-micaschists show a clastic texture, with detrital quartz and coarse grained mica embedded in a fine grained quartz - chlorite - sericite matrix.

Chloritoid-bearing phyllites: they crop out as less than 10 cm thick layers in the sequence, interbedded within the carbonate ± chlorite micaschists. These rocks, violet to whitish in colour, are characterized by a slaty cleavage and under the microscope show a strongly foliated structure, mostly composed of extremely fine

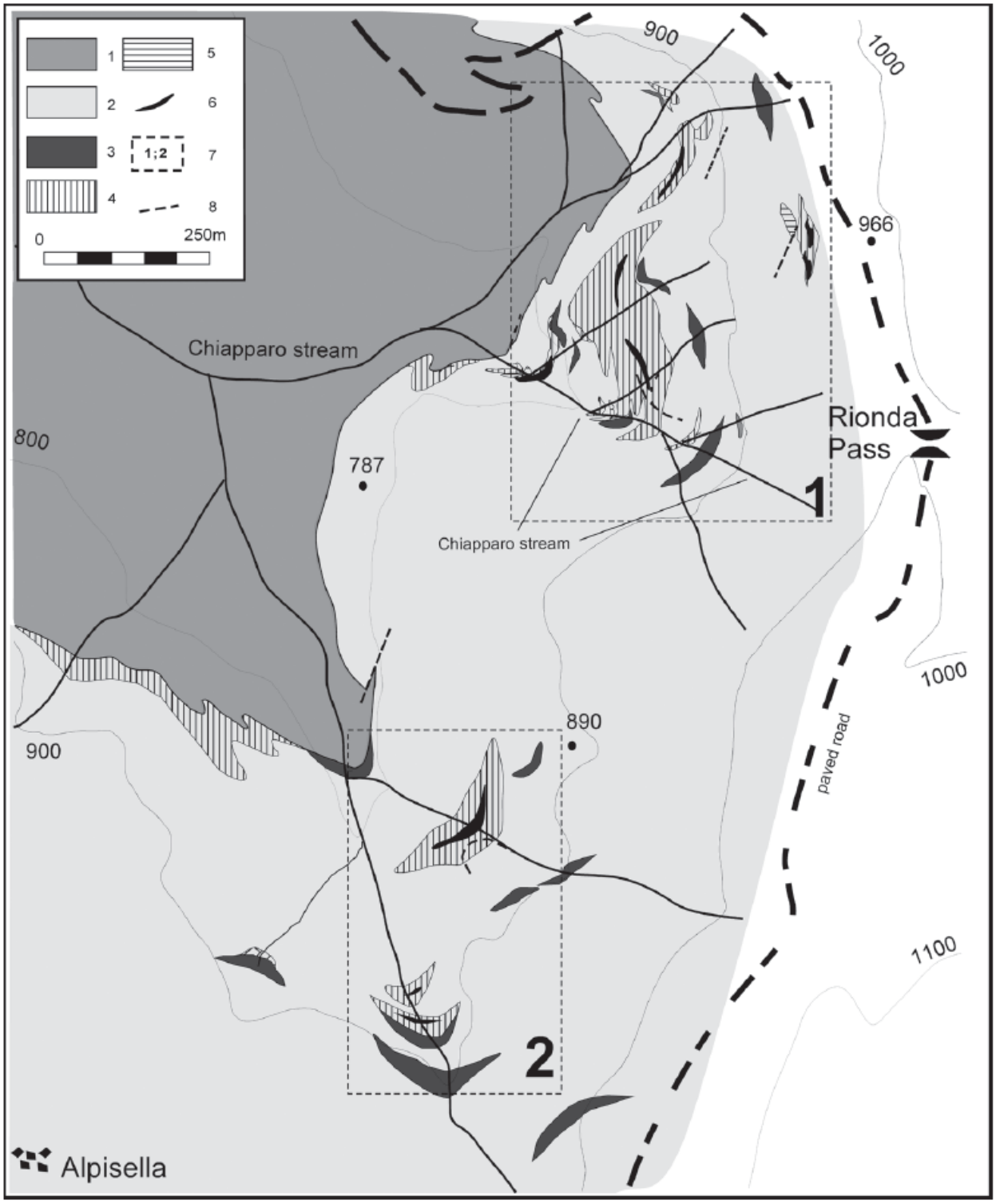

Fig. 3: Interpretative geological map of the Casario area, based on 1:5000 mapping. **1:** Murialdo Formation (indifferentiated); **2:** Gorra Schists s.s., with interlayered albite-micaschists and chloritoid-bearing phyllites; **3:** lawsonite-pumpellyite phyllites and albite porphyroclasts-bearing schists (*Eze Formation Auct.*); **4:** chloritoid – carbonate micaschists; **5:** carbonatic schists and silicate marbles; **6:** main massive sulphide bodies. **7:** location of the main mineralized areas (Area 1 and Area 2; a detail of Area 1 is shown in Fig. 6). **8:** faults.

grained white mica and quartz. The violet colour is related to the abundance of very fine grained rutile and chloritoid (the latter as up to 500 microns big crystals, pre- to synkinematic to S_2). Chlorite overgrows white mica. The whitish varieties, slightly coarser grained, are enriched in carbonate.

Within the Gorra Schists, the following rock-types occur, shown in Figs. 3 and 5:

Carbonatic schists and silicate marbles: they occur as scattered, up to few metres thick lenses, light green to dark grey in colour. The *carbonatic schists* show a foliated fabric, being mainly composed of quartz - carbonate domains alterned with thinner mica-rich levels. Carbonate can be very fine grained or recrystallized to poikiloblasts enclosing quartz and rutile; it also occurs, with rutile, as replacement of abundant clastic ilmenite. Quartz mostly forms porphyroclasts (at least in part deriving from detrital quartz) or finer grained intergrowths in pressure shadows around pyrite grains. Some rounded albite also occurs. The same rocks pass laterally, with increasing carbonate content, to *silicate marbles*, composed of the same phases.

Lawsonite - pumpellyite phyllites and *albite porphyroclasts-bearing schists*: they crop out as up to 50 m thick and several tens of metres long, lens-shaped, intercalations of very fine grained, massive green rocks at different levels within the Gorra Schists. These rocks, which are mapped together in Figs. 3 and 5, correspond to the green rocks described in the Literature as “prasinite” (i.e., greenschist facies metabasite) belonging to the Eze Formation [19].

The *lawsonite - pumpellyite phyllites* contain metamorphic assemblages which can help to constrain the metamorphic evolution of the Gorra Schists; for this reason a detailed petrologic study has been carried out, also based on SEM-EDS and MicroRaman spectroscopy analyses.
Under the microscope these rocks show an extremely fine grained oriented fabric, mainly composed of quartz, white mica and chlorite. The microstructural observations allow recognition of different metamorphic assemblages. A first assemblage is represented by lawsonite, as relict nematoblasts oriented along S_1, associated with very fine grained pumpellyite (I) (confirmed by MicroRaman spectroscopy: Fig. 4), fine grained phengitic mica (Si = 3.45 atoms pfu: Table 1), chlorite and albite. This assemblage occurs as a relic, being overgrown by a new association characterized by the unoriented growth of all new phases. The new assemblage is given by abundant pumpellyite (II, X_{Mg}: 0.59), chlorite (X_{Mg} = 0.48, Table 1), phengitic mica (Si = 3.38 atoms pfu: Table 1) and albite; lawsonite is clearly unstable. Pumpellyite (II) composition is similar to that reported from meta-andesite in the Murialdo Formation [31].
A third assemblage is represented by very fine grained chlorite + titanite ± white mica growing along the S_2 planes. Quartz and accessory titanite are at equilibrium in all the assemblages; abundant very fine grained rutile occurs as a relic partially transformed to titanite, the two often replacing primary ilmenite.

Albite porphyroclasts-bearing schists: they show a spaced and anastomosed foliation, alternating chlorite - white mica-rich and quartz-feldspatic domains. The latters show a broadly lenticular shape and are composed of coarse grained albite embedded by quartz. Albite occurs both as pre-F_1 porphyroclasts, often strongly sericitized, and as a later phase, locally rimming early albite and enclosing quartz and white mica. Along the foliation white mica is often deeply transformed to chlorite; calcite and ankerite also occur. Rutile, zircon, apatite and rare rounded pyrite are accessory. The abundance of porphyroclasts of albitized plagioclase suggests for these rocks a possible derivation from a reworked pyroclastic to volcanoclastic material (crystal tuff?).

C*hloritoid – carbonate micaschists*: these rocks mostly crop out, as discontinuous bodies, along a broadly N-S oriented horizon, some tens of metres above the contact with the Murialdo Formation (Figs. 3 and 5), which envelopes the massive sulphide lenses. The interpolations of the field and petrographic observations suggest the occurrence, within Area 1, of an at least 300 m long, up to 40-50 m thick body of chloritoid – carbonate micaschists. Minor lenses not directly associated with the mineralizations crop out in the lower part of the Gorra Schists, at the contact with the Murialdo Formation.
These rocks, light green to whitish in colour, range from medium- to fine grained and are composed of interbedded, millimetre-thick, quartz-rich and chloritoid-rich layers; up to few centimetres sized quartz clasts locally occur. They are often flooded by milky quartz veinlets parallel to the S_1 foliation, displaying folds with acute hinges. The contact with the host rocks is sharp.

In the chloritoid – carbonate micaschists the dominant assemblage is represented by quartz + chloritoid + white mica (muscovite-phengite) ± carbonate ± pyrite ± sphalerite; tourmaline, fine grained rutile and zircon are accessory.

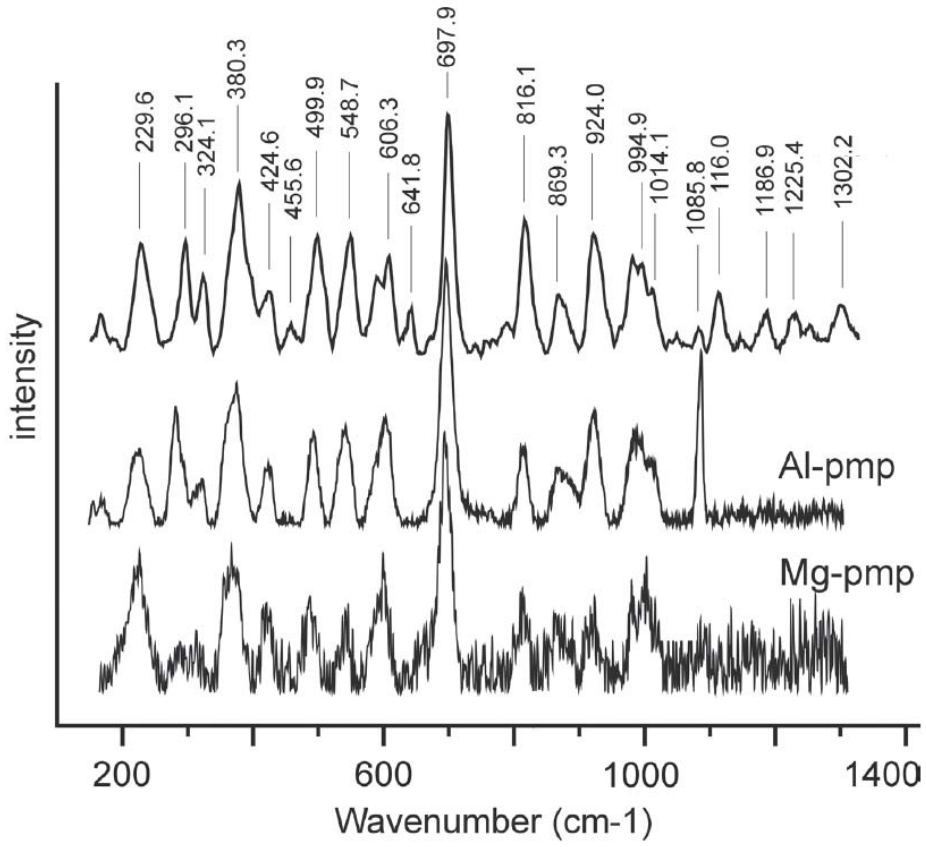

Fig. 4: MicroRaman spectrum of pumpellyite (I) from lawsonite-pumpellyite phyllite compared with Al- and Mg-pumpellyite from the RRUFF™ Raman database [30]. These analyses have been performed in order to obtain an unambiguous phase determination: in fact, due to the very small grain size, SEM-EDS mostly gave mixed analyses. Shifts in peak positions among the different spectra depend on mineral composition (particularly, X_{Mg}), while differences in relative intensities are mainly function of mineral orientation relative to the incident polarized laser beam. MicroRaman spectroscopy was performed with a LabRAM-HR 800 (HORIBA - JOBIN-YVON) spectrometer at the Dipartimento di Scienze Mineralogiche e Petrologiche, University of Torino, Italy, using a Nd solid state laser (532 nm, 100 mW).

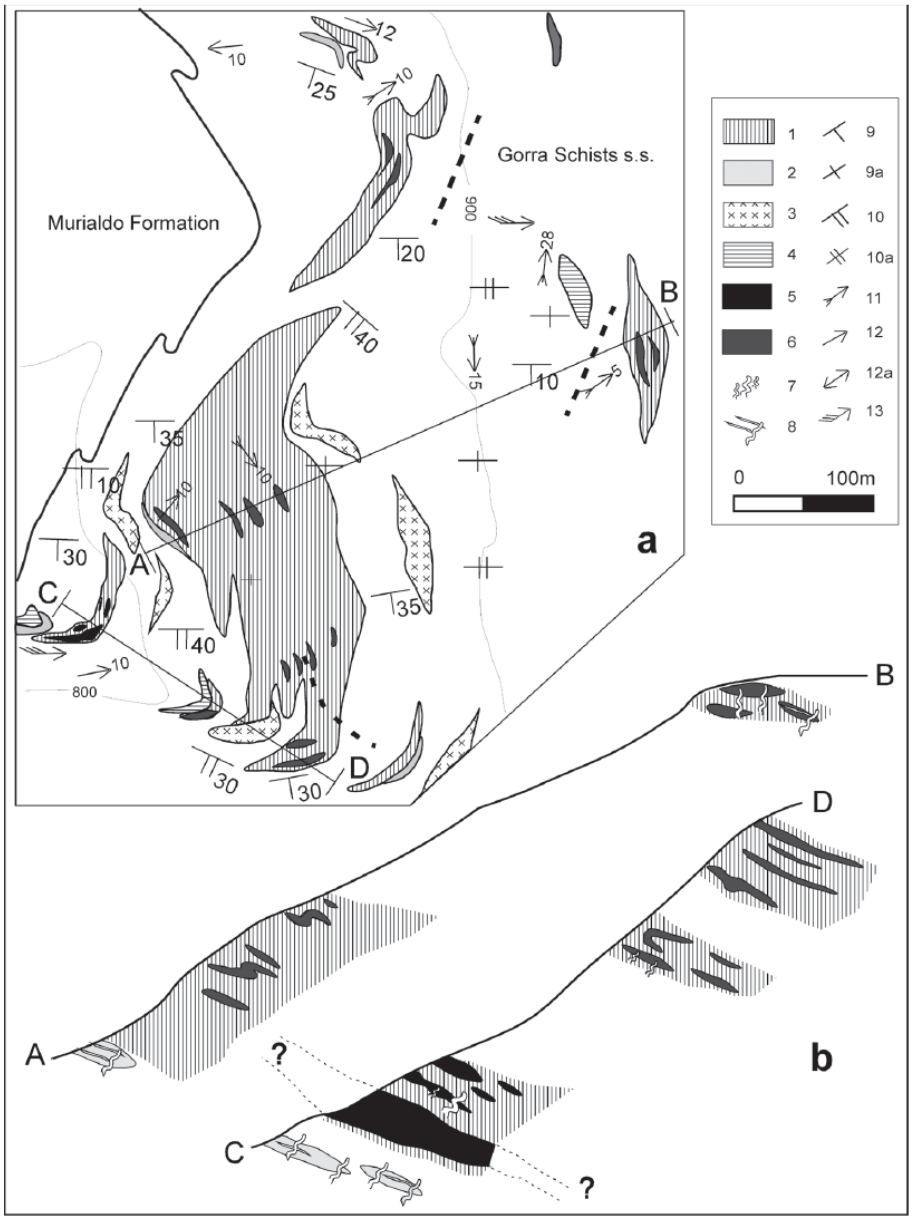

Fig. 5: a: interpretative geological map of Area 1. The Murialdo Formation and Gorra Schists s.s. are shown in white. **1:** chloritoid – carbonate micaschists; **2:** sulphide-rich quartz – carbonate - chloritoid granofels; **3:** lawsonite-pumpellyite phyllites and albite porphyroclasts-bearing schists (*Eze Formation Auct.*); **4:** carbonatic schists and silicate marbles; **5:** sphalerite-galena massive sulphide lenses; **6:** pyrite-rich lenses. Structural data: **9:** S_1 (9a: sub-horizontal), **10:** S_2 (10a: sub-horizontal), **11:** F_1 axes, **12:** F_2 axes (12a: sub-horizontal), **13:** F_3 (sub-horizontal) axes. The sulphide-rich lenses are enlarged for clarity. **b:** highly schematic cross sections showing the geometric position of the sulphide-rich bodies (enlarged for clarity) and hydrothermal veins. Rock symbols as in Fig. 5a. 7, 8: deformed hydrothermal veins cross-cutting S_0 within the massive sulphide lenses and/or the chloritoid – carbonate micaschists (7) and the sulphide-rich quartz – carbonate - chloritoid granofels (8).

A peculiar character of these rocks is the common occurrence of a finely bedded texture, with sharp between-bed compositional contrast (Fig. 6), defined by interbedding of chloritoid-layers (and/or white mica) with quartz-rich layers. Quartz is the most abundant phase, as fine grained intergrowths in monomineralic beds; clastic quartz grains also occur. Other phases can be highly variable, even at the thin section scale. Chloritoid (10-25% range) often occurs as up to some hundred microns-thick layers, even associated with white mica; it is always a Fe end-member and in some beds contains some Mn (up to 2 wt% MnO: Table 1). Within the beds, chloritoid occurs as fine grained crystals parallel to the compositional layering (which generally also corresponds to the S_1 foliation), or as radiated intergrowths of prismatic to needle-shaped crystals, which suggest post-F_1 static growth (Fig. 7). Locally radial, needle-shaped chloritoid overgrows coarser grained and strongly fractured prismatic crystals; the two generations show the same Fe-rich composition. A white mica rim locally bounds chloritoid. Within monomineralic beds or together with chloritoid, phengitic mica (Si = 3.30-3.35 atoms pfu: Table 1) is associated with minor paragonite. A second generation of white mica develops along the S_2 foliation planes, with a lower celadonite content (Si = 3.15 atoms pfu: Table 1). Carbonate (magnesite-siderite solid solution: Table 2) highly varies, from 0% to 10-20%; it occurs as isolated grains associated with quartz or, more often, along thin beds. When present, chlorite (X_{Mg}: 0.48, Table 1) is concentrated along thin beds parallel to the compositional layering, often associated with fine grained pyrite and minor chalcopyrite; the latters also grow along the S_2 planes.

Anhedral sphalerite also occurs within quartz ± carbonate domains. Tourmaline, rutile, zircon, apatite are accessory phases.

5. The sulphide deposits

The sulphide deposits (Figs. 3 and 5) occur as strongly flattened bodies (lenses and boudins) with a thickness ranging from 10 to 100 cm; single bodies can be traced in the outcrops for no more than few metres along the creeks and their lateral extent is buried by the Quaternary cover. The F_1 phase is responsible of tight to isoclinal folds, and has locally transformed the lenses into a series of boudins (Fig. 8). The F_2 cleavage is less evident than in the host schists, both in the field and under the microscope; F_3 affects the attitude of the whole sequence, included the sulphide lenses. Based on the sulphides abundance, two main types of mineralizations can be recognized: massive sulphide lenses and sulphide-rich quartz – chloritoid schists.

5.1. Massive sulphide lenses

The lenses occur in the northern and central part of the area (Figs. 3 and 5), closely associated with the chloritoid – carbonate micaschists and characterized by a sulphides content exceeding 50% (up to around 90%). Two types of massive sulphide lenses can be recognized: sphalerite - galena massive lenses and pyrite-rich lenses. Along the Chiapparo creek a strong compositional change occurs, from lenses with dominant sphalerite and galena in the geometrically lower part of the sequence to lenses strongly enriched in pyrite in the upper part (Fig. 5).

5.1.1. Sphalerite - galena massive lenses

The sphalerite - galena massive lenses occur both in Area 1 and 2 (Figs. 3 and 5), where can reach a thickness of around 40 cm and a lateral extent along the outcrops up to few metres; the average sulphides content is around 70%. The lenses show a strong centimetric compositional layering, with layers from few millimetres up to 6-7 cm thick composed of thinly laminated sphalerite and/or galena alternating with pyrite-rich layers (Fig. 9). Within and/or between the sulphides-rich layers, quartz – carbonate concentrations occur, as centimetre-sized irregularly- to lens-shaped domains parallel to the layering.

Under the microscope the main components are sphalerite, galena, pyrite, arsenopyrite, carbonate, chloritoid and quartz, with minor chlorite, white mica, tetrahedrite, pyrrhotite and chalcopyrite.

Within the Zn-Pb-rich beds both sphalerite and galena mostly occur thin layers which can be monomineralic or, more often, are composed of fine grained sphalerite or galena enclosing a minor amount of all other phases. Under transmitted light (Fig. 9) sphalerite is transparent, yellowish to light brown in colour, as typical of low-Fe sphalerite (4.5 to 8.0 mol% FeS: Table 2); after etching both sphalerite and galena show a well developed annealed structure (Fig. 10).

Pyrite occurs within both sphalerite- and galena-rich layers, mostly as coarse grained (up to few millimetres), strongly fractured porphyroclasts (Figs. 9 and 11) containing small inclusions of pyrrhotite; sphalerite, galena, tetrahedrite and very minor chalcopyrite often occur along the cracks in pyrite (Fig. 11), and locally appear to replace it. Arsenopyrite is mostly represented by fine grained

Table 1: Representative composition of silicates from different rock types of the Casario area.

	Phe1	Phe2	Phe3	Phe4	Phe5	Pmp	Ctd1	Ctd2	Ctd3	Pg	Chl1	Chl2	Chl3	Carph
SiO_2	49.88	48.52	47.01	44.43	47.27	37.57	24.35	23.94	24.39	47.32	26.22	24.40	24.00	38.71
TiO_2	0.00	0.00	0.40	0.00	0.00	0.00	0.00	0.00	0.00	0.00	0.00	0.00	0.00	0.00
Al_2O_3	25.83	25.91	27.92	32.05	36.21	24.34	38.08	40.05	40.38	39.90	19.60	23.40	27.34	32.58
FeO_{tot}	2.58	4.07	3.27	2.40	0.75	3.53	28.89	25.04	25.04	0.00	27.16	29.24	28.82	8.29
MnO	0.00	0.00	0.00	0.00	0.00	0.70	0.00	1.93	1.32	0.00	0.47	0.92	0.70	0.64
MgO	3.10	3.55	1.65	0.47	0.69	3.37	1.73	1.25	1.54	0.00	14.07	10.50	7.32	7.78
CaO	0.00	0.00	0.00	0.00	0.00	23.65	0.00	0.00	0.00	0.00	0.00	0.00	0.00	0.00
Na_2O	0.00	0.00	0.43	0.50	1.15	0.00	0.00	0.00	0.00	6.38	0.00	0.00	0.00	0.00
K_2O	10.79	10.05	10.26	10.05	8.62	0.00	0.00	0.00	0.00	1.26	0.00	0.00	0.00	0.00
Total	92.18	92.10	90.94	89.90	94.69	93.15	93.05	92.21	92.67	94.86	87.52	88.46	88.18	88.00
Oxygens	11	11	11	11	11	24.5	12	12	12	11	28	28	28	10
Si	3.449	3.379	3.312	3.151	3.117	6.001	2.030	2.004	2.025	3.023	5.614	5.255	5.227	2.012
Ti	0.000	0.000	0.021	0.000	0.000	0.000	0.000	0.000	0.000	0.000	0.000	0.000	0.000	0.000
Al	2.105	2.127	2.318	2.678	2.814	4.583	3.742	3.951	3.952	3.004	4.946	5.940	7.018	1.996
Fe^{2+}_{tot}	0.149	0.237	0.193	0.142	0.041	0.471	2.014	1.753	1.739	0.000	4.864	5.267	5.249	0.360
Mn	0.000	0.000	0.000	0.000	0.000	0.095	0.000	0.137	0.093	0.000	0.085	0.168	0.129	0.028
Mg	0.320	0.369	0.173	0.050	0.068	0.802	0.215	0.156	0.191	0.000	4.491	3.371	2.376	0.603
Ca	0.000	0.000	0.000	0.000	0.000	4.048	0.000	0.000	0.000	0.000	0.000	0.000	0.000	0.000
Na	0.000	0.000	0.059	0.069	0.147	0.000	0.000	0.000	0.000	0.790	0.000	0.000	0.000	0.000
K	0.952	0.893	0.922	0.909	0.725	0.000	0.000	0.000	0.000	0.103	0.000	0.000	0.000	0.000
X_{Mg}	0.682	0.609	0.474	0.259	0.621	0.586	0.096	0.076	0.094	-	0.476	0.383	0.306	0.608

Lawsonite-pumpellyite phyllites: Phe1, Phe2: Stage I and II (see also Fig. 18) muscovite–phengite, respectively; Pmp: Stage II pumpellyite; Chl1: Stage II chlorite. Chloritoid – carbonate micaschists: Phe3, Phe4: Stage I and III muscovite-phengite, respectively; Ctd1, Ctd2: Fe-chloritoid; Chl2: Stage I chlorite in chlorite-rich beds. Sphalerite-galena lenses, Stage I+II: Phe5: muscovite; Ctd3: Fe-chloritoid; Chl3: chlorite; Pa: paragonite. Carph: carpholite from the quartz-calcite-carpholite veins.

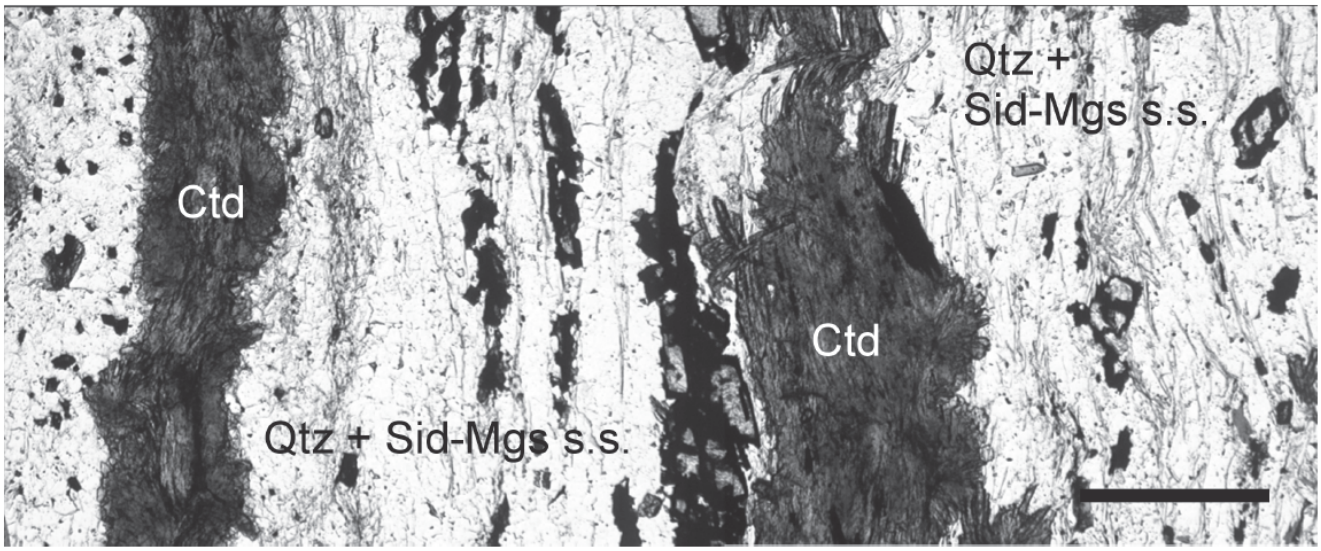

Fig. 6: Finely bedded texture of the chloritoid – carbonate micaschists (see text for details). Qtz-quartz, Ctd-chloritoid, Sid-Mgs s.s.- siderite-magnesite s.s. Plane polarized transmitted light, bar width: 0.5 cm.

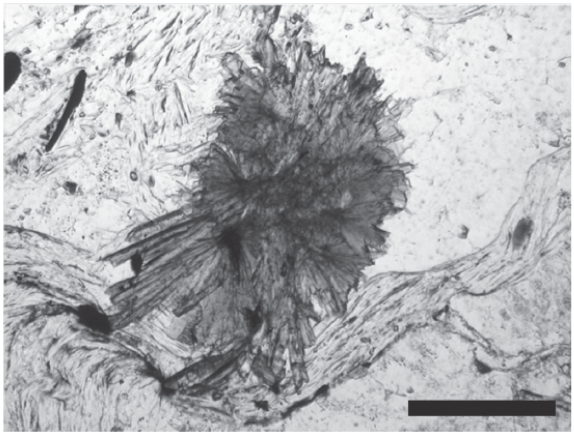

Fig. 7: Radial growth of Fe-chloritoid in the chloritoid – carbonate micaschists. Plane polarized transmitted light, bar width = 200 microns.

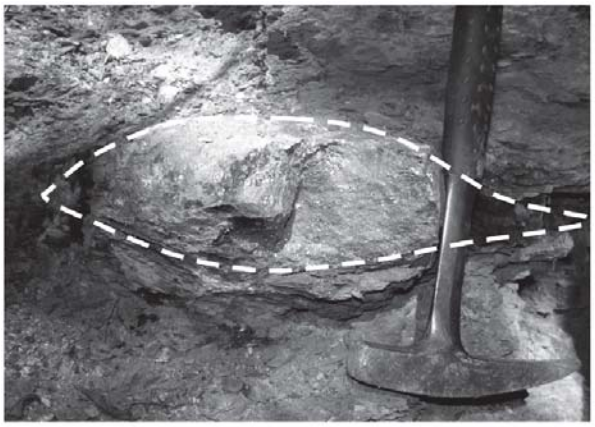

Fig. 8: Massive sulphide lens strongly boudinaged by F_1. Upper Chiapparo stream, west of Rionda Pass.

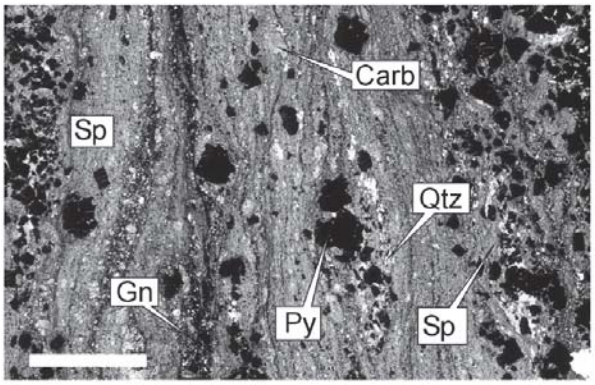

Fig. 9: Compositional layering of the Zn-Pb lenses. Abundant sphalerite (Sp, grey) interbedded with minor layers of galena (Gn, black fine grained material) within a Zn-rich bed; fine grained quartz (Qtz, here mainly clastic) and carbonate (Carb) also occur. Pyrite (Py, black grains) occurs in highly variable amount, and is locally concentrated along some layers (right and left in the photo); in the Zn-rich layers (central part of the photo) it forms porphyroclasts embedded by sphalerite and galena. Transmitted light, bar width = 0.5 cm.

sub-euhedral to anhedral crystals closely associated with pyrite, locally enclosing sphalerite and galena which may also occur in arsenopyrite microcracks.

Within low strain domains, fine grained pyrite and arsenopyrite in the Zn-rich domains locally display a strong rhythmic zoning: pyrite shows primary growth zones enriched in As (up to 3.5 wt.%), while associated arsenopyrite displays Sb enrichments (up to 3.0 wt.%; Fig. 12). In deformed domains, such growth zoning is absent: pyrite becomes coarser grained and homogeneous, and arsenopyrite composition varies only in terms of Fe, As and S contents (Table 2).

The pyrite-rich beds are mostly composed of coarse grained euhedral pyrite associated with minor arsenopyrite; tetrahedrite, galena, sphalerite and chalcopyrite occur, in very minor amount, along microcracks in pyrite.

The gangue broadly shows the same mineral assemblage of the chloritoid - carbonate micaschists. Carbonate (siderite – magnesite – rhodochrosite s.s.: Table 2) is the most abundant phase, as irregularly shaped grains within elongated domains parallel to the S_1 foliation. Quartz occurs both as clasts and as finer grained crystals; it is generally interstitial to the sulphides and also occurs as elongated fibres in pressure shadows around pyrite. Needle-shaped crystals of chloritoid, locally abundant, occur along chloritoid-rich domains parallel to the rock bedding and as radial intergrowths in the sulphides rich domains, where it shows equilibrium relationships with sphalerite and galena. Chloritoid composition is close to the pure Fe end member (Table 1); when associated with sphalerite it may display a low Zn content (up to 0.9 wt.%). White mica can form very fine grained intergrowths or, alternatively, coarser grained crystals associated with carbonate, quartz and locally sphalerite. It is mostly represented by muscovite, slightly enriched in Na, with a low celadonite content (Si = 3.10-3.19 atoms p.f.u.); paragonite may also occur (Table 1). Chlorite mostly forms thin, discontinuous domains parallel to the bedding; it shows the lowest X_{Mg} (= 0.31, Table 1).

5.1.2. Pyrite-rich lenses

The pyrite-rich lenses are particularly abundant in Area 1, where occur as lens-shaped bodies enclosed in the chloritoid – carbonate micaschists; they crop out in the geometrically higher part of the sequence, above the Zn-Pb bodies (Fig. 5). These lenses show a variable structure, from massive to slightly layered; total sulphides content ranges from 40% to around 70%.

In these lenses pyrite is the dominant phase (up to 90% of sulphides), mostly as euhedral crystals with grain size variable from few tens of microns to one centimetre; it is locally associated with arsenopyrite and often contains inclusions of sphalerite and pyrrhotite. Tetrahedrite (silver-bearing, Sb-rich: Table 2), chalcopyrite and galena or, alternatively, arsenopyrite and sphalerite occur along microcracks in pyrite. Sphalerite also occurs as porphyroclasts, locally

Table 2: Representative composition of carbonates and sulphides from the Casario area.

	Sid1	Sid2	Sid3	Sid4		Sp1	Sp2	Td	Apy1	Apy2
FeO_{tot}	45.61	35.37	32.31	44.86	S	32.59	32.20	25.21	21.19	23.31
MnO	1.21	10.33	10.97	1.74	Mn	0.00	0.93	0.00	0.00	0.00
MgO	10.08	9.43	13.63	7.61	Fe	2.57	4.62	5.62	35.41	36.48
CaO	0.00	0.56	0.31	0.81	Cu	0.00	0.00	38.32	0.00	0.00
Total	56.90	55.69	57.22	55.02	Zn	64.51	62.71	0.00	0.00	0.00
					As	0.00	0.00	4.31	42.10	40.19
Fe^{2+}_{tot}	1.408	1.117	0.949	1.467	Ag	0.00	0.00	2.98	0.00	0.00
Mn	0.038	0.330	0.326	0.058	Sb	0.00	0.00	23.01	0.00	0.00
Mg	0.554	0.530	0.713	0.443	Total	99.67	100.45	99.45	98.71	99.98
Ca	0.000	0.023	0.012	0.034						
X_{Mg}	0.277	0.268	0.359	0.225	Mn	0.000	0.017	0.000	0.000	0.000
					Fe	0.045	0.082	1.663	0.959	0.899
					Cu	0.000	0.000	9.972	0.000	0.000
					Zn	0.971	0.955	0.000	0.000	0.000
					As	0.000	0.000	0.951	0.850	0.738
					Ag	0.000	0.000	0.457	0.000	0.000
					Sb	0.000	0.000	3.125	0.000	0.000
					FeS at%	4.49	8.01			

Chloritoid – carbonate micaschists: Sid1: siderite-magnesite s.s. Sphalerite-galena lenses: Sid2, 3: siderite-magnesite-rhodochrosite s.s.; Sp1, Sp2: sphalerite; Apy1, 2: coarse grained arsenopyrite. Pyrite-rich lenses: Sid4: siderite-magnesite s.s.; Td: tetrahedrite s.s. Carbonates are recalculated on the basis of 2 cations; sulphides on the basis of: sphalerite, arsenopyrite: 1, tetrahedrite: 13 S atoms. Minerals were analyzed with a Cambridge Stereoscan 360 scanning electron microscope (SEM) equipped with an energy-dispersive spectrometer (EDS) at the Dipartimento di Scienze Mineralogiche e Petrologiche, University of Torino, Italy. The operating conditions were: 50 s counting time and 15 kV accelerating voltage. Microprobe data were acquired and managed using the Microanalysis Suite Issue 12, INCA Suite version 4.01; the raw data were calibrated on natural mineral standards and the ZAF correction method was applied.

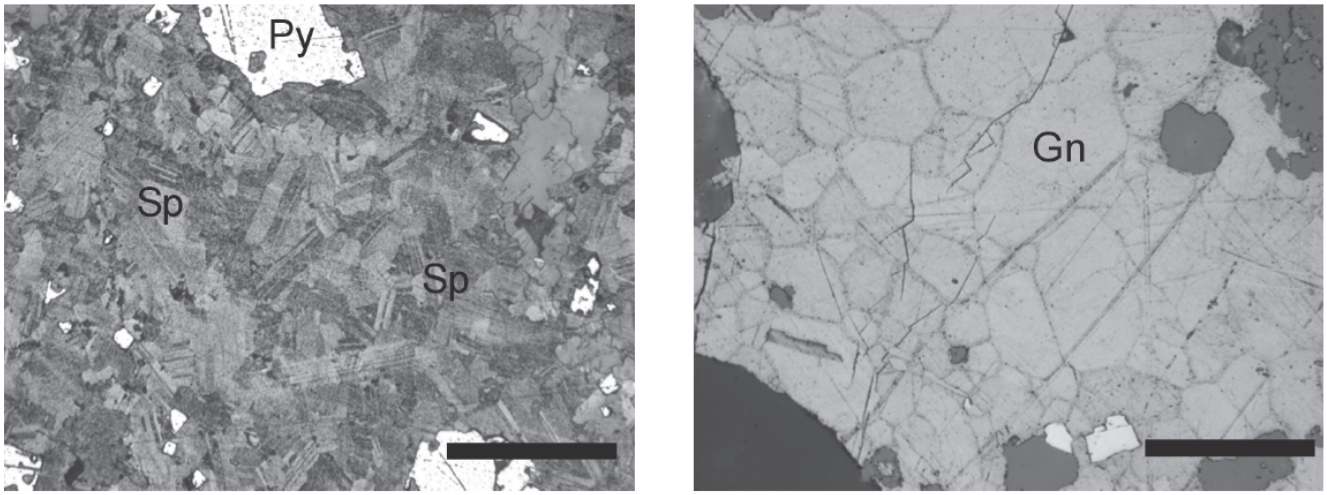

Fig. 10: Sphalerite- (**a,** at left) and galena-rich (**b** at right) domains in the sphalerite-galena lenses after etching with HCl. a: sphalerite patches enclose corroded pyrite (bright white) and are composed of a polycrystalline sub-equigranular intergrowth of crystals showing polysynthetic twinning. Plane polarized reflected light, bar width = 100 microns. b: galena shows a "foam" texture composed of sub-equant, polygonal grains with triple-junction angles averaging 120°. Plane polarized reflected light, bar width = 50 microns.

displaying some compositional zoning (with a darker, Fe-enriched rim); minor galena forms irregular patches embedding all other phases.
Gangue is composed of carbonate (siderite – magnesite s.s.: Table 2), quartz, Fe-chloritoid, white mica and chlorite: they show the same characters than those described for the sphalerite-galena lenses. A compositional layering is locally observed, with alternating pyrite-rich and quartz – carbonate layers.

An important character of the pyrite-rich lenses is the occurrence, within undeformed domains, of *relict textures***.**
A common relict texture is represented by the occurrence in pyrite of a spongy core, surrounded by fine grained recrystallized pyrite (Fig. 13a); the latter may also occur along microcracks. Locally both spongy core and outer rim are crosscut by thin veinlets filled with sphalerite, arsenopyrite, tetrahedrite, galena and minor chalcopyrite. Spongy cores are generally made of very fine grained pyrite only; more rarely they are composed (as shown by SEM-EDS analyses) of an extremely fine grained intergrowth of pyrite and galena. These spongy textures are never observed in even slightly deformed domains, where homogeneous, euhedral pyrite occurs instead.
Another relict texture is represented, still in undeformed pyrite-rich domains, by clast-supported microbreccias composed of up to few millimetres sized angular clasts embedded in a quartz + Fe-Mg carbonate + pyrite + sphalerite hydrothermal matrix. The clasts are not oriented and consist of fine grained pyrite + quartz + carbonate, often displaying a thinly bedded structure; they are in part surrounded by a thin rim composed of euhedral pyrite. Within the clasts pyrite occurs as few microns-sized grains, mostly sub-parallel to the bedding, but also as coarser grained crystals, which overgrow the sedimentary protolith; some clasts are wholly composed of coarse grained pyrite, suggesting that the pyrite enrichments are related, at least in part, to replacement phenomena (Fig. 13b).

5.2. Sulphide-rich quartz – carbonate - chloritoid granofels

Sulphides concentrations also occur, in both Area 1 and 2, within quartz – carbonate - chloritoid granofels which crop out as scattered dark lenses up to 10 m thick, generally associated with the chloritoid - carbonate micaschists. These rocks show a compositional layering, broadly parallel to the S_1 foliation.

Under the microscope these rocks show strong similarities with the chloritoid – carbonate - quartz micaschists associated with the massive sulphide lenses: the mineral assemblage is, in fact, the same, the main difference being the abundance of sulphides (up to 50%), quartz and carbonate, and a lower content of white mica, chloritoid and chlorite; as a consequence, the rock texture is much more isotropic than the schists. A compositional banding is often observed, with millimetre- to centimetre-thick layers alternatively enriched in sulphides ± chloritoid, quartz + carbonate and white mica ± chlorite. Quartz is very fine grained, probably deriving from cherty material.
Sulphides are mainly concentrated along up to few centimetres-thick layers and consist of sub-euhedral to euhedral pyrite with variable amounts of sphalerite, galena and tetrahedrite. Like in the pyrite-rich lenses, pyrite with spongy core and recrystallized rim occurs. Sphalerite is locally abundant, concentrated along thin layers which also contain fine grained euhedral pyrite and anhedral galena; the latter may contain irregularly shaped tetrahedrite and also fills microfractures in pyrite.

A peculiar character of the sulphide-rich quartz – chloritoid schists is the occurrence of pyrite-rich veinlets (up to 1 cm thick) which crosscut the primary bedding. These veinlets consist of quartz, carbonate and pyrite (the latter coarser grained than in the host rock) and are not surrounded by any reaction rim; they show a microbrecciated texture, with unoriented clasts of finely bedded quartz-carbonate-pyrite embedded in very fine grained quartz-rich matrix. These veinlets locally spread out laterally into sulphide-rich layers, suggesting a connection with an exhalative activity.

6. Veins within the Gorra Schists

Different types of veins occur within the Gorra Schists, namely:

Quartz – carbonate – sulphides hydrothermal veins. These veins crop out in different parts of the area within the Gorra Schists, especially close to the sulphide lenses. They can be up to around 10 cm thick and often crosscut at high angle the primary bedding (S_0), but are affected by the F_1 deformation, which generates cylindric hinges whose geometry is consistent with S_1 (Fig. 14). These relationships, which suggest a pre-deformation emplacement of the veins, are seen within the chloritoid – carbonate micaschists and the lawsonite – pumpellyite phyllites; within more

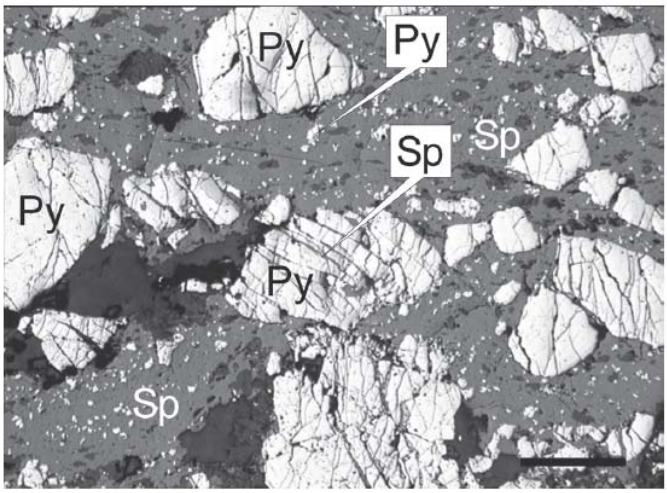

Fig. 11: Typical aspect of pyrite within the sphalerite-galena lenses (see text for more details). Plane polarized reflected light, bar width = 1mm

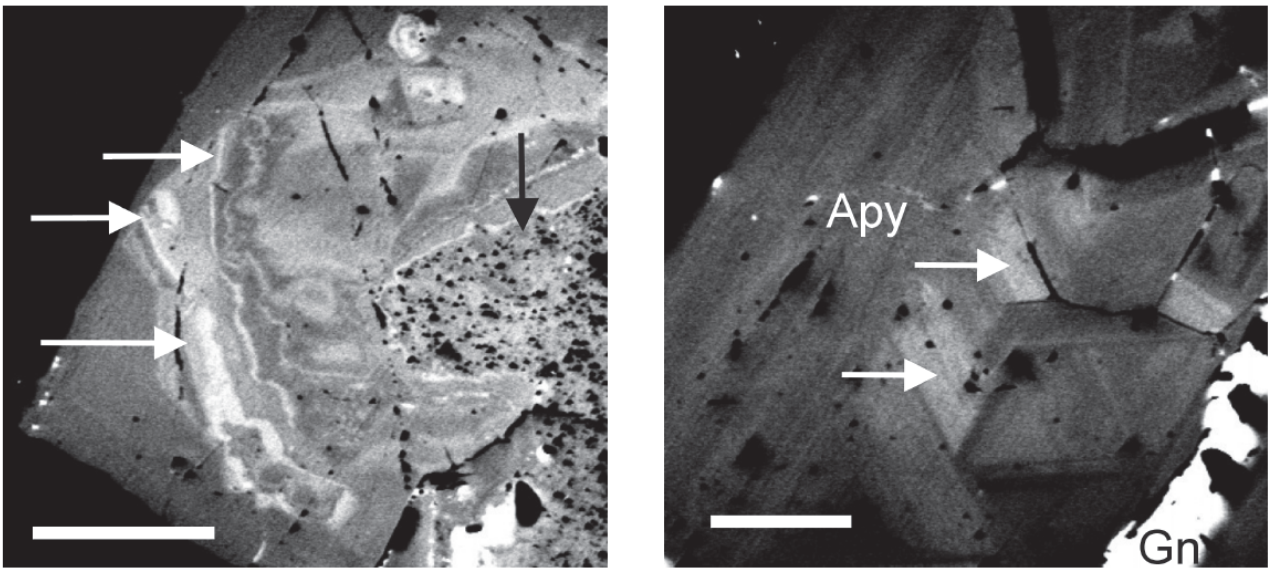

Fig. 12: (**a** at left)**:** Pyrite in undeformed sphalerite-galena lens showing primary zoning, with thin growth zones (lighter in the photo: white arrows) enriched in As. The zoned pyrite surrounds an older grain composed of pyrite and very fine grained quartz + carbonate (black arrow: quartz-carbonate-pyrite clast?). SEM backscattered image, bar width: 100 microns. (**b** at right)**:** Arsenopyrite grain associated with pyrite of Fig. 12a. Arsenopyrite shows a primary zoning, with areas (white arrows, lighter in the photo) enriched in Sb. Arsenopyrite is here crosscut by later galena (Gn). SEM backscattered image, bar width: 25 microns.

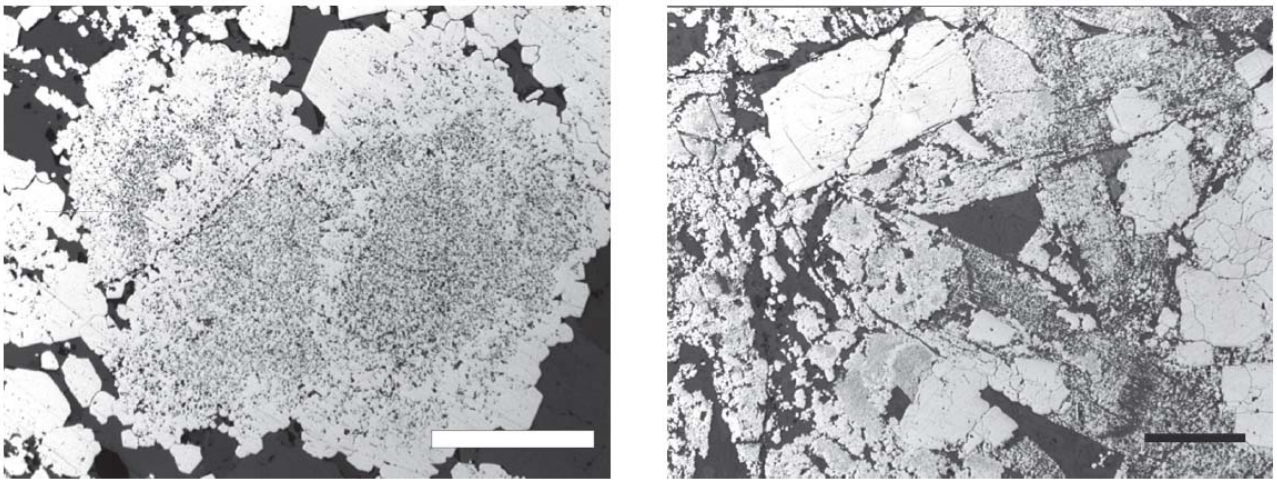

Fig. 13: (**a** at left)**:** Relic, spongy pyrite core rimmed by recrystallized pyrite within the pyrite-rich lenses. Plane polarized reflected light, bar width = 200 microns. (**b** at right)**:** Pyrite-rich, clast-supported microbreccia from the pyrite-rich lenses. Clasts are strongly enriched in pyrite (white), which occurs both as very fine grained intergrowths with quartz and carbonate (grey) and as coarser grained crystals, which also overgrow the contact between clasts (lower centre). Some clasts (upper left and right) have been completely replaced by coarse grained pyrite. Plane polarized reflected light, bar width = 1 mm.

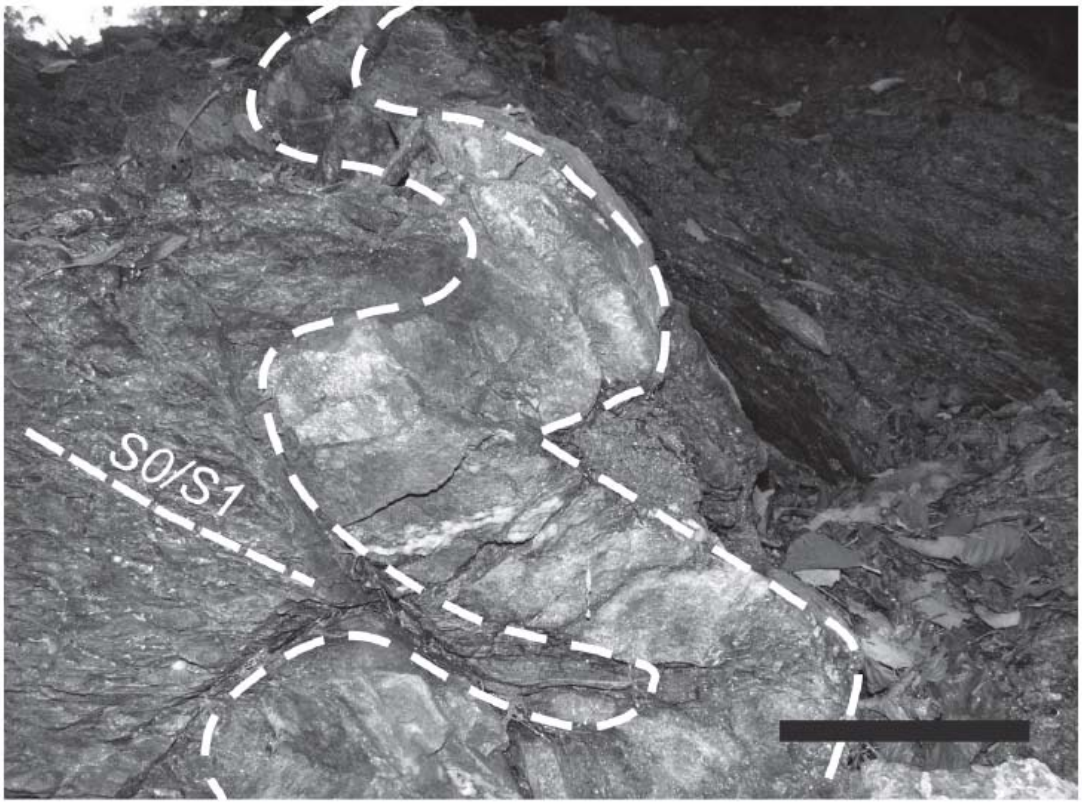

Fig. 14: Quartz – carbonate – sulphides hydrothermal vein. The vein crosscuts the primary bedding of the host chloritoid-carbonate micaschists and is strongly deformed by the F_1 phase, which generates tight folds with axial plane sub-parallel to S_1. Area 1, NW of Rionda Pass. Bar width = 15 cm.

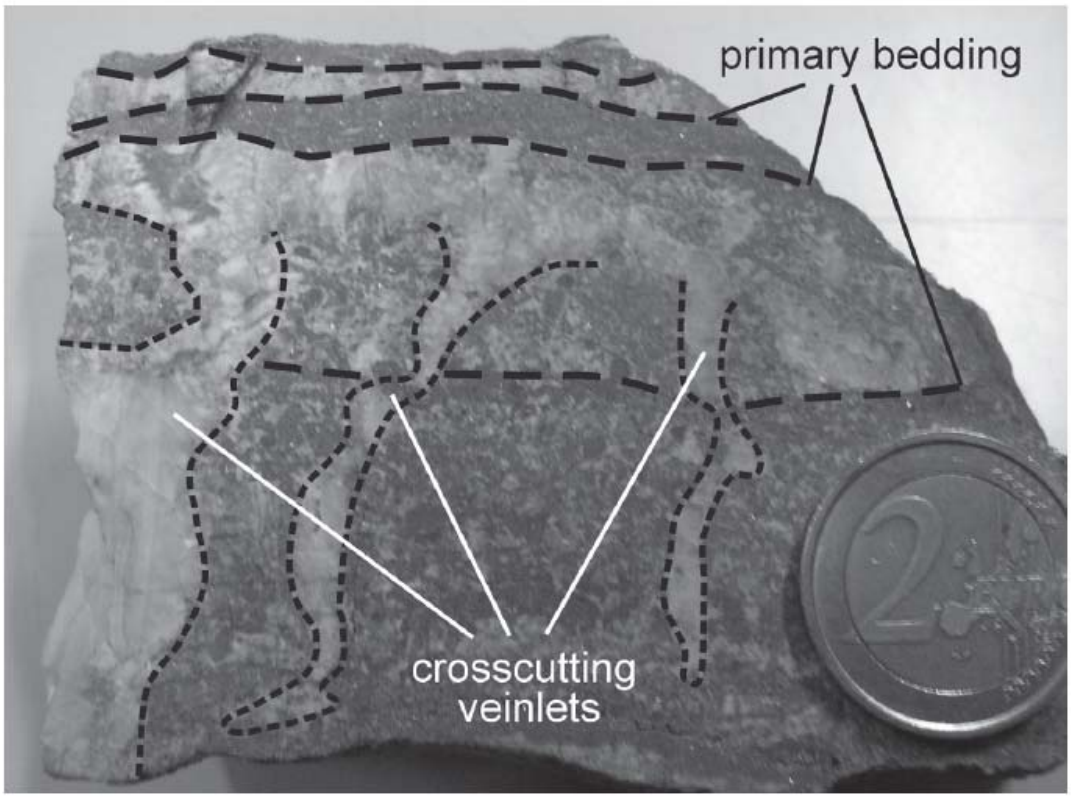

Fig. 15: Irregularly-shaped quartz – carbonate – sulphides veinlets crosscut the primary bedding of a pyrite-rich lens. The veinlets terminate upwards and spread out laterally into a quartz-carbonate-sulphide layer, suggesting a close relationship with the exhalative activity. Area 1, NW of Rionda Pass.

ductile rock types, veins with the same composition are strongly discontinuous and sub-parallel to the foliation.
Under the microscope these veins are composed of quartz and Fe-Mg carbonate, with minor amounts of sulphides (pyrite, galena and very minor chalcopyrite) and Fe-Mg chlorite. Similar veins are also found within the sulphide lenses: particularly, NW of Rionda Pass, within Area 1 (Figs. 3 and 5) quartz – carbonate + minor pyrite and sphalerite veins crosscut bedded pyrite-rich bodies and are, in turn, truncated by quartz-sulphides beds (Fig. 15).

Quartz + calcite + carpholite veins. They only occur in clasts along the Chiapparo stream; however, the composition of the associated stream sediments suggests the Gorra Schists as a source area. The veins, up to 10 cm thick, are strongly deformed, and characterized by the occurrence of light green, acicular carpholite crystals of up to several centimetres in length.
Under the microscope the veins are composed of coarse grained quartz and calcite. Needles of carpholite (Mg-carpholite: X_{Mg} = 0.608, Table 1) are included in quartz.
The occurrence of carpholite has been recently reported in several localities of the Western Alps, and is considered as a typical phase of high pressure - low temperature metamorphic conditions [32, 33]. In the Ligurian Alps, carpholite occurs abundantly in the Brianconnais Zone, both in the Upper Carboniferous - Permian schists and in the Mesozoic cover [34 and references therein]; its occurrence is related to the alpine metamorphic peak.

Quartz ± ankerite veins. Quartz ± ankerite veins, up to 10 cm thick, are common in the Gorra Schists. At least two types of veins occur: (i) discontinuous, flattened quartz veins parallel to the S_1 foliation, or as relict hinges of isoclinal folds; (ii) quartz or quartz + ankerite veins crosscutting the S_1 foliation and deformed by the later folding phases.

7. Metamorphic evolution of the Gorra Schists

Both Gorra Schists and sulphide lenses record a polyphase metamorphic evolution of alpine age developed under low- to very low grade conditions, as already recognized for this sector of the Briançonnais Zone [17]. In order to better constrain the conditions of the metamorphic overprint, a petrologic study has been performed of selected rock-types, by calculating a *P-T* pseudosection at fixed bulk-rock composition.

The petrologic study has been performed on the lawsonite-pumpellyite phyllites, because they are very fine grained, homogeneous rocks which contain multiphase assemblages that record a polyphase evolution. In fact, based on the microstructural observations, the following main assemblages, corresponding to metamorphic stages (earlier to later) are recognized:
I) *lawsonite + pumpellyite + white mica + chlorite + albite + quartz + titanite*
II) *pumpellyite + white mica + chlorite + albite + quartz + titanite*
III) *chlorite + titanite ± white mica*
The bulk composition was obtained by analyzing, by SEM-EDS, five 4.70 x 3.20 mm areas and considering the average as representative composition (i.e., by adopting the method of Groppo *et al.* [35]). Based on the obtained bulk composition, a pseudosection in the system Al_2O_3-CaO-FeO-K_2O-MgO-Na_2O-SiO_2-TiO_2–H_2O was calculated following the approach of Connolly [36], and using the internally consistent thermodynamic data set and equation of state for H_2O of Holland and Powell (1998, upgrade 2002 [37]). Chlorite, glaucophane and phengite solid-solutions have been used in the calculation; albite was considered as pure end-member. As no carbonate occurs in the studied samples, H_2O was considered as the only fluid phase affecting mineral equilibria.
The pseudosection, calculated in the range T = 150 – 400°C, P = 0.2 - 0.8 GPa, is shown in Fig. 16. In the pseudosection, Stage I and II assemblages (fields 1 and 2, respectively) occur over a range of P-T conditions comprised between P = 0.32-0.79 GPa and T= 200-330°C. Main boundary conditions are, at high P and low T, the absence of glaucophane, and at low P the absence of microcline, laumontite and/or prehnite. An upper T limit is given by the absence of clinozoisite and biotite.
Further constraints are given by the location of the phengite isopleths in the two fields (Fig. 17). The celadonite content of phengitic mica ranges from Si = 3.45 atoms p.f.u. when associated with lawsonite (Stage I) to slightly lower (Si = 3.38 atoms p.f.u.) in Stage II pumpellyite-rich domains post-dating lawsonite. These data constrain the P-T conditions of Stage II assemblage at around P = 0.55-0.60 GPa, T = 300-325°C; Stage I is instead poorly constrained, as the phengite isopleths in this field are sub-parallel to the boundary between Stage I and II assemblages.
In order to further constrain the lower T limit of Stage I, a pseudosection calculation has been performed on a chloritoid – carbonate micaschist

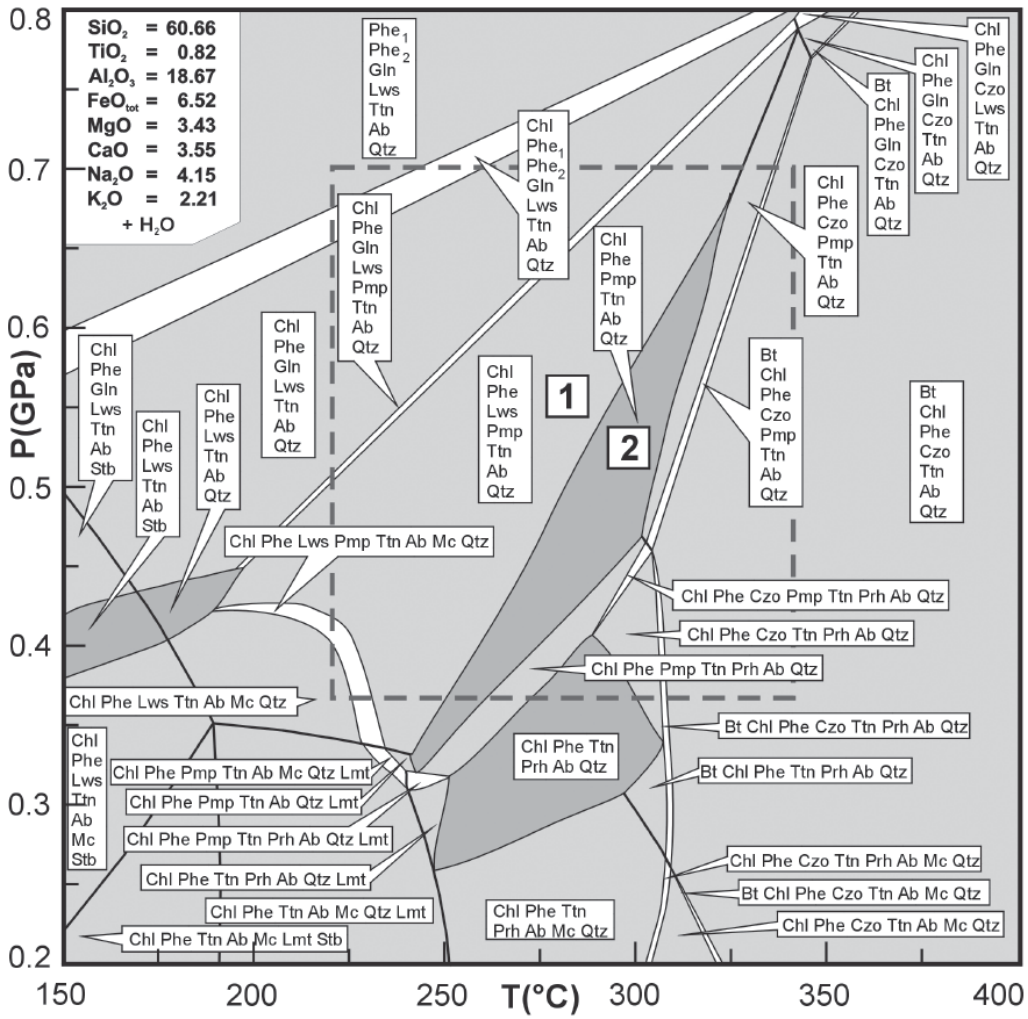

Fig. 16: Pressure-temperature (P-T) pseudosection for the lawsonite – pumpellyite phyllites calculated in the Al_2O_3-CaO-FeO-K_2O-MgO-Na_2O-SiO_2-TiO_2–H_2O system for the bulk composition (recalculated to 100%) shown in the top right inset. Dark-grey, light-grey and white fields are quadri-, tri- and divariant fields, respectively. Thick lines are discontinuous reactions. Mineral abbreviations according to [38]: Ab-albite; Bt-biotite; Chl-chlorite; Czo-clinozoisite; Gln-glaucophane; Lmt-laumontite; Lws-lawsonite; Mc-microcline; Phe-phengite (Phe_1, Phe_2: phengites of different composition coexistent at high P); Pmp-pumpellyite; Prh-prehnite; Qtz-quartz; Stb-stilbite; Ttn-titanite. 1 and 2 refer to Stage I and II assemblages, respectively. The dashed rectangle shows the area enlarged in Fig. 17.

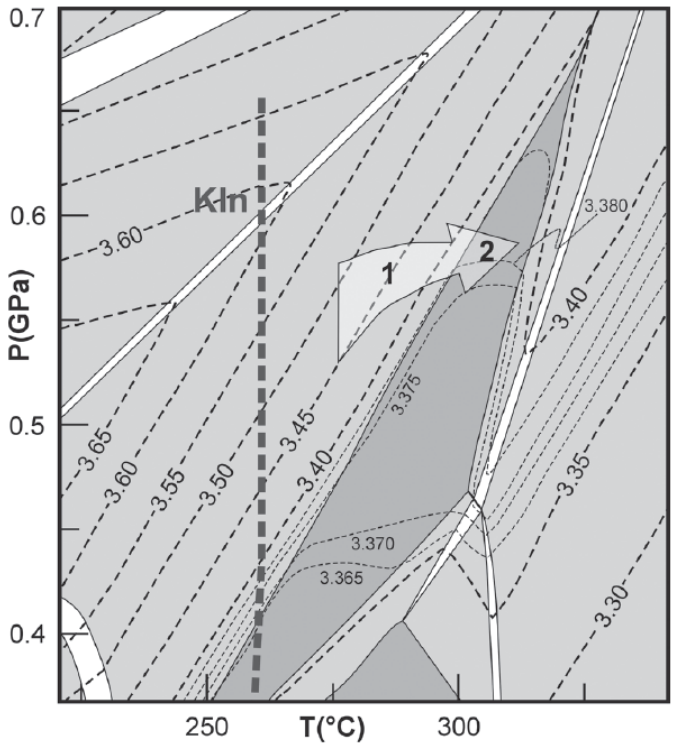

Fig. 17: Enlargement of the central portion of Fig. 16, with reported (dashed lines) the phengite isopleths (as Si atoms p.f.u.). The thick dashed line shows the upper stability conditions of kaolinite (Kln) in the chloritoid-carbonate micaschists (see text). The arrow shows the inferred prograde metamorphic evolution (1: Stage I; 2: Stage II) of the lawsonite-pumpellyite phyllites.

within domains devoid of carbonate. The pseudosection is not shown, as it only displays (due to the rock composition) wide high variance fields; however, the strongly T-dependent stability field of Fe-chloritoid + phengite *without* kaolinite (which does not occur in these rocks: dashed curve in Fig. 17) provides a minimum T limit of around 260°C for the development of Stage I assemblage.

By combining the calculated P-T pseudosections with the petrologic observations, P-T conditions of 0.55-0.60 GPa can be inferred for Stage II assemblage, which is likely to represent the climax metamorphic conditions for the Gorra Schists. Stable I assemblage probably developed at slightly lower P-T conditions (P ~ 0.53-0.57 GPa, T = 270-290 °C), during the prograde evolution (arrow in Fig. 17). The post-peak evolution (Stage III) is instead poorly constrained, as only represented by few phases crystallized along cleavage planes and, due to the low-T conditions, a well developed re-equilibration is not observed. In the chloritoid – carbonate micaschists, decreasing P conditions are suggested by the much lower celadonite content of potassic mica (Si ~ 3.15 atoms p.f.u.).

The calculated P-T conditions are in agreement with the data of Messiga [39], who suggests for the Pamparato – Murialdo Unit pressure values ranging from 0.4 to 0.6 GPa and temperatures not exceeding 400°C.

8. Discussion

8.1. Age of the massive sulphide lenses

The mineralizations of the Casario area consist of lenses of massive Zn-Pb-Fe sulphides interbedded within the Gorra Schists. The structural observations show that they were affected by all the ductile deformation phases recorded in the host sequence; this is in agreement with the petrologic study, which stresses the occurrence of a metamorphic overprint in the sulphide lenses. Moreover, they locally still record a pre-metamorphic history, which is discussed below. Several features, like the stratiform shape of the sulphide bodies, the finely bedded character of the sphalerite – galena lenses, their occurrence within a narrow stratigraphic interval and the close association with pre-metamorphic hydrothermal veins, strongly suggest an exhalative origin for the deposits. Even in case of sulphides concentrations precipitated during a subsurface replacement event, like probably the pyrite-rich microbreccias and possibly part of the pyrite-rich lenses (see below), their timing of formation was “synsedimentary” (i.e. during the early stages of sediment diagenesis: [40]). The emplacement of the sulphide bodies occurred during the deposition of the host Gorra Schists, of inferred upper Stephanian age [8]: an Upper Carboniferous age is therefore suggested for the exhalative-sedimentary event.

8.2. Pre-metamorphic features of the sulphide lenses

In spite of the tectono-metamorphic reworking, pre-metamorphic features connected with the massive sulphides emplacement are still locally preserved.

8.2.1. Pre-metamorphic hydrothermal veins

Within the Gorra Schists, the quartz – carbonate – sulphides veins often observed close to the massive sulphides, which display crosscutting relationships with the host bedding but are affected by all the deformation phases, represent pre-metamorphic hydrothermal veins. A clear genetic relationship with the sulphide bodies is the occurrence, within the veins, of Fe-Mg carbonate and sulphides (particularly, sphalerite), as in the sulphide lenses. These data make them interpret as part of hydrothermal feeding system.
Within undeformed domains of the pyrite-rich lenses, pre-metamorphic veins locally crosscut the primary bedding and spread out laterally into sulphide-rich layers, as expected in an exhalative environment. At the microscale, thin sulphides-rich veinlets commonly occur crosscutting early formed pyrite, suggesting a complex and prolonged hydrothermal activity as often documented in the massive sulphide deposits from different settings [e.g., 41, 42, 43, 44, 5].

8.2.2. Relict textures in the sulphide bodies

Different types of relict, possibly pre-metamorphic textures are still preserved in undeformed portions of the sulphide bodies.

Within the *sphalerite – galena lenses* a primary feature is represented by the compositional growth zoning locally displayed by pyrite and associated arsenopyrite, which contain growth zones of sure primary origin enriched, respectively, in arsenic and antimony. Similar zoning patterns in pyrite have been documented from ore deposits of different origin, including massive sulphide deposits, where strong Au concentrations are often observed in the As-rich domains (e.g., 45). Sb-enrichments in (gold-rich) arsenopyrite are also locally reported, mostly from mesothermal deposits [46, 47]. Primary compositional zoning in pyrite can be preserved even in strongly metamorphosed deposits [48]; at

Casario it has been instead mostly obliterated during an early recrystallization stage, possibly due to sulphur exchange with other sulphides [48]. The occurrence of abundant pyrite porphyroclasts deformed by F_1 also suggests an early, pre-metamorphic recrystallization stage.

In the *pyrite-rich lenses*, a relict texture of possible primary origin is represented by extremely fine grained, spongy cores in pyrite, rimmed by recrystallized pyrite. The absence of these textures in even slightly deformed domains suggests their pre-metamorphic character. These cores could tentatively be interpreted as relics of early-formed poorly crystalline, very fine grained, pyrite, even if unambiguous evidences of collomorphic or framboidal pyrite, often reported from massive sulphide deposits [e.g., 49, 50, 51], have not been found.

Based on the microstructural study, also the spongy pyrite + galena intergrowths pre-date deformation and metamorphism. Their significance is unclear: in massive sulphides from different settings galena generally does not occur in primary growth textures with pyrite (though primary pyrite-galena intergrowths are locally reported: [52]). As pyrite is crosscut by hydrothermal sulphides-bearing veinlets, fine grained galena could also be related to impregnation (and/or partial replacement) of spongy pyrite by later fluids.

A surely pre-metamorphic feature is represented by sulphide-rich microbreccias, composed of pyrite-enriched clasts embedded in a quartz - Fe-Mg carbonate - pyrite ± sphalerite hydrothermal matrix. The microstructural observations suggest that the strong pyrite enrichments in the clast are the product of replacement phenomena.

8.3. The bedded chloritoid-rich schists: meta-exhalites associated to the massive sulphide lenses

Fe-chloritoid-rich schists are closely associated with the massive sulphide lenses. These rocks show a peculiar assemblage and composition (being strongly enriched in silica and almost completely devoid of sodium and calcium); but the most striking character of at least part of them is their finely bedded texture, with sharp between-bed compositional contrast. The bedding is affected by all the deformation phases and is surely a primary character.

Several features, namely: *a)* the close association with the massive sulphide lenses; *b)* the finely bedded texture, with sharp contrast between Al- and silica-rich beds; *c)* the occurrence of siderite-magnesite s.s., which is the typical composition of carbonate in and around the massive sulphide lenses at Casario; *d)* the presence of sulphides (mainly pyrite and sphalerite) enrichments along the beds, particularly approaching the sulphide lenses; *e)* the occurrence of MnO enrichments in the Fe-chloritoid from some beds, suggest that these rocks represent meta-exhalites, i.e., the metamorphic product of rocks whose finely bedded texture is related with the exhalative activity. The primary compositional layering of exhalites is, in fact, often well preserved in metamorphic rocks, even affected by high grade metamorphic overprint [53].

8.4. Constraints on the hydrothermal evolution

In spite of the tectono-metamorphic overprint, the geologic and petrologic observations allow a partial reconstruction of the hydrothermal evolution. In the field, the Murialdo Formation always lies below the younger Gorra Schists. In the latters, the sphalerite-galena massive sulphides occur close to the base of the sequence, and the pyrite-rich bodies overlie them. These observations suggest that at the scale of the unit the stratigraphic setting is broadly preserved and doublings related to the F_1 phase are of only local importance. The observed compositional variations from the lowest to the highest part of the series are, therefore, likely to represent changes of the exhalative activity through time.

In the sphalerite-galena lenses, deposition developed a rhythmic layering, with alternating millimetre- to centimetre-thick galena-rich and sphalerite-rich layers. Associated pyrite and arsenopyrite initially grew (Fig. 18) as fine grained crystals, at least locally with rhythmic compositional zoning (with As and Sb enrichments, respectively) which probably reflect subtle changes in fluid composition during deposition. During a subsequent stage, pyrite and arsenopyrite recrystallized to homogeneous crystals (*rexx* in Fig. 18). Particularly, pyrite recrystallized to coarser grained crystals which now occur as porphyroclasts whose formation pre-dates deformation and metamorphism. Tetrahedrite and chalcopyrite generally occur, in low strain domains, along crosscutting veinlets (often associated with galena and sphalerite), suggesting a relationship with a relatively late hydrothermal stage. Pyrrhotite is rare, only occurring as inclusions within pyrite porphyroclasts; it could have formed during, or just before, the early recrystallization stage.

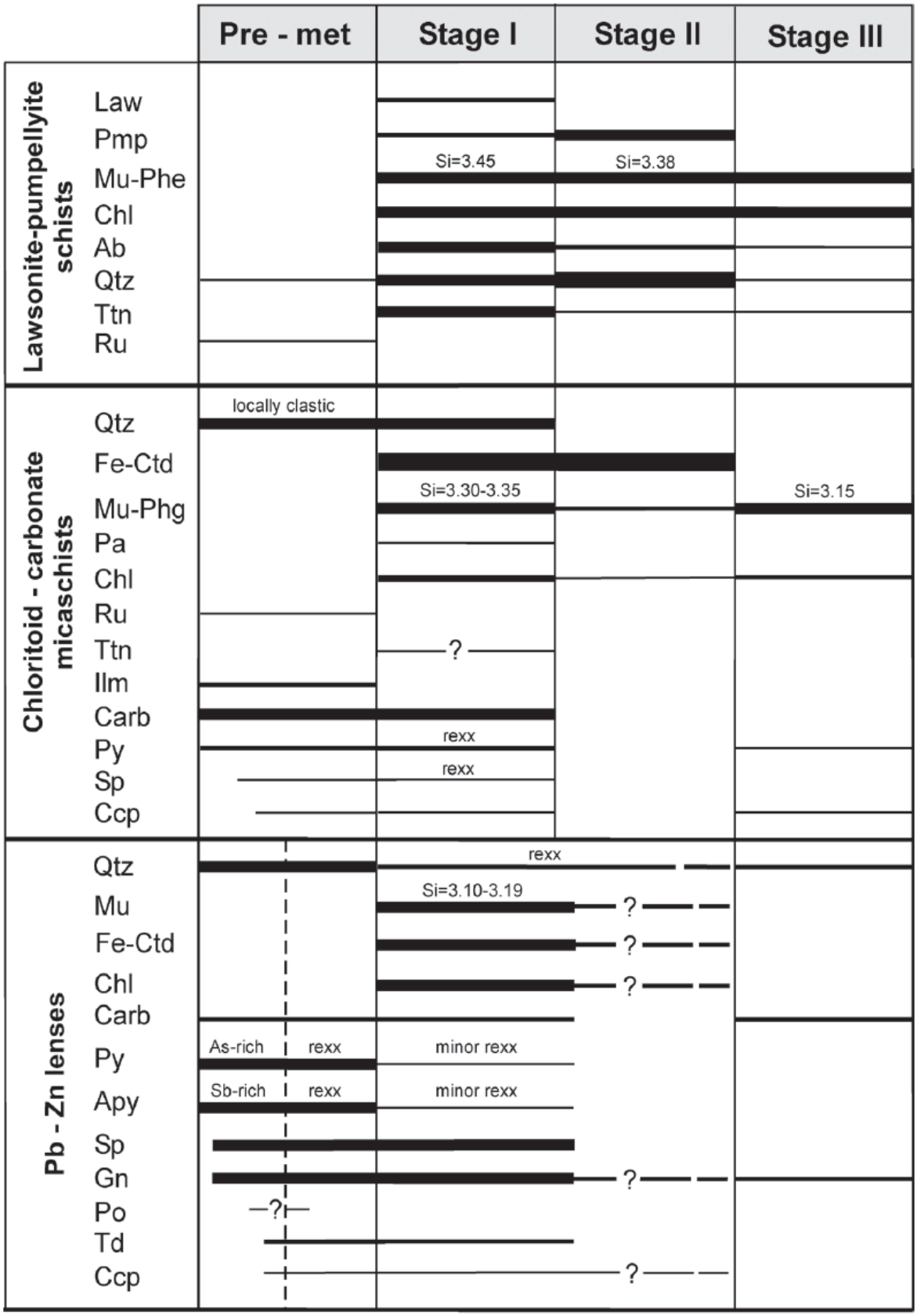

Fig. 18: Inferred pre-metamorphic and metamorphic evolution for selected rock-types of the Gorra Schists and Zn-Pb lenses. Rexx: recrystallization. The lines thickness broadly relates to average mineral abundance. Same mineral symbols of Figs. 9 and 16, other symbols: Mu-muscovite; Ru-rutile; Fe-Ctd - Fe-chloritoid; Pa-paragonite; Ilm-ilmenite; Ccp-chalcopyrite; Po-pyrrhotite; Td-tetrahedrite s.s.

Within the pyrite-rich lenses, an early crystallization stage is represented by extremely fine grained, spongy pyrite, which during a subsequent stage mostly recrystallized to fine- to relatively coarse-grained euhedral crystals; both pyrite generations are crosscut by sphalerite – arsenopyrite – tetrahedrite – galena - chalcopyrite hydrothermal veinlets. Evidences of replacement in at least part of the pyrite-rich bodies is documented in the clasts-supported microbreccias. At present it is unclear to which extent replacement occurred in the system. It must be noted, however, that strong replacement could probably produce rocks like the pyrite-rich bodies.

In both types of sulphide-rich lenses, pyrite (and arsenopyrite in the sphalerite-galena lenses) record an early, pre-deformation recrystallization stage, which could be tentatively related to diagenetic transformations, as suggested for other massive sulphide deposits [e.g., 54].

8.5. Classification of the Casario massive sulphide deposits

The massive sulphide lenses of the Casario area occur within a stratigraphic succession mostly composed of siliciclastic sediments with interbedded a very minor volcanic (l.s.) component, represented by the lawsonite - pumpellyite phyllites and albite porphyroclasts-bearing schists, related to the andesitic magmatism; a close correlation between magmatic rocks and sulphide deposits is not observed.

The overall characters of the deposits, coupled with the absence of a strict connection with the coeval magmatism, suggest that the Casario deposits may be classified as SEDEX (sedimentary-exhalative: [55, 56, 57]) deposits; this would also be in agreement with the very high (Pb+Zn)/Cu ratio, which is generally much lower in the VMS (volcanic-associated massive sulphide: [1, with references]) deposits. A high Cu content would be, in particular, expected in case of a relationship with the andesitic magmatism [1, 4]; at Casario the mineralization consists instead of strong Zn and Pb (-Ag) enrichments, with Cu-bearing sulphides only occurring in very minor amount.

More data are needed in order to characterize the anatomy of the system. It is worth noting, however, that the sphalerite-galena lenses show strong analogies with the "*bedded ore facies*" of the SEDEX deposits [43]; the finely layered structure of the Zn-Pb mineralization, with alternating sphalerite- and galena-rich layers, and its association with interbedded quartz (at least in part deriving from chert) – carbonate concentrations, suggest that they represent sea floor hydrothermal sediments.

The significance of the pyrite-rich lenses is in part unclear. Pyrite-rich microbreccias show evidences of replacement, suggesting a sub-surface environment of sulphides formation; at least part of the coarse-grained massive pyrite-rich lenses could also be related to hydrothermal replacement. The occurrence of brecciated structures, replacement phenomena, and crosscutting relationships between early-formed pyrite and sulphide-bearing veinlets shows similarities with the "massive pyrite facies" reported at different levels of the "*vent complex*" from some well studied SEDEX deposits (e.g., Jason, Selwyn Basin, Canada: [5, with references therein]).

The finely bedded chloritoid-rich schist, interpreted as meta-exhalites, may correspond to the "*distal sedimentary facies*" and/or layers of sedimentary - exhalative material in the post-ore series overlying the sphalerite-galena lenses [43].

The pre-metamorphic quartz – carbonate – sulphides veins observed close to the massive sulphides within the Gorra Schists are likely to represent a relic of the hydrothermal feeding system. The paucity of sulphides within the veins, as often documented in the SEDEX deposits, strongly contrasts with the VMS deposits, which are typically characterized by feeding veins strongly enriched in sulphides, especially chalcopyrite [5].

8.6. Metamorphic evolution of the Gorra Schists and sulphide lenses

The Gorra Schists and sulphide lenses record a polyphase metamorphic evolution, which is tentatively resumed in Fig. 19.

As already discussed, the *lawsonite-pumpellyite phyllites* record a multiphase evolution. A first lawsonite + pumpellyite-bearing assemblage (Stage I) is followed by a pumpellyite-bearing, lawsonite-absent association (Stage II); Stage II is characterized by the static growth of pumpellyite. A third stage (Stage III) is testified by growth of muscovite, chlorite and titanite along the S_2 planes.

In the *chloritoid – carbonate micaschists* showing a well developed exhalite texture (Fig. 19), quartz, Fe-Mg carbonate, sulphides (pyrite and sphalerite ± chalcopyrite) and clastic rutile and/or ilmenite were surely part of the pre-metamorphic assemblage, together with Al-rich, probably argillaceous material. During an early stage (Stage I) Fe-chloritoid, phengitic mica, some paragonite and chlorite formed, in highly variable proportions strongly depending on the primary

beds composition; quartz, carbonate and sulphides also recrystallized, at least in the deformed domains. Stage II is clearly shown by the static growth of a second generation of Fe-chloritoid, post-dating F_1; at least some muscovite-phengite (and possibly also other phases) probably recrystallized during this stage, even if microstructural relationships are not clear. A third stage (Stage III) is represented by growth of new mica (with low celadonite content) and, in beds enriched in primary sulphides disseminations, very fined grained pyrite ± chlorite ± chalcopyrite along the S_2 planes.

The effects of the metamorphic overprint on the sulphide bodies are less obvious: particularly, the available data do not allow a clear recognition of a Stage I and Stage II assemblage in the sulphide lenses, but only a Stage I+II (Fig. 19), characterized by the crystallization of muscovite-phengite, Fe-chloritoid, chlorite and recrystallization of carbonate and quartz. Sphalerite and galena at least in part recrystallized, as shown by the equilibrium relationships with Fe-chloritoid (and muscovite); their present microfabric, though surely attained through a long-lasting annealing process probably begun even before the onset of metamorphism, probably reflect, at least in high strain domains, the attainment of equilibrium at peak metamorphic conditions [58, 59]. Chalcopyrite and (at least in part) tetrahedrite also recrystallized. Pyrite and arsenopyrite were instead transformed to strongly fractured porphyroclasts, whose cracks are filled with sphalerite, galena, tetrahedrite and chalcopyrite. Stage III is even less evident: only locally, cataclastic planes crosscutting at high angle the S_1 foliation, filled with very fine grained calcite, quartz and minor galena, could be related to the effects of the S_2 deformation.

9. Conclusions

The Zn-Pb (-Ag) deposits of Casario represent the product of sedimentary – exhalative processes which occurred during the deposition of the Upper Carboniferous Gorra Schists. The geological setting and the overall characters suggest a SEDEX affiliation for the massive sulphide deposits, which in low strain domains still show, in spite of the tectono-metamorphic overprint, features related to their pre-alpine evolution, like primary growth and replacement textures, relics of the feeding system and evidences of an early (possibly diagenetic) recrystallization event.

The exhalative bodies and host schists have been affected by a lower greenschist facies alpine metamorphism (climax conditions: P = 0.55-0.60 GPa, T = 300-325 °C) accompanied by different phases of ductile deformation.

The petrologic study stresses the difference in behaviour between massive sulphides and host schists during the alpine history. Massive sulphide lenses only partially record the multistage alpine overprint; particularly, pyrite and arsenopyrite mostly behaved as refractory phases during the metamorphic evolution. The latter is instead much better recorded within the host rocks. This difference in behaviour is due to the “refractory” behaviour of pyrite and arsenopyrite [60, 48], and to the contrast in rheology between massive sulphides and host schists: deformation and related fluid circulation more deeply affected the strongly ductile schists, thus promoting the onset of metamorphic reactions, while the sulphide lenses were only partially re-equilibrated.

The exhalative activity developed during the Upper Carboniferous, characterized by the occurrence of shallow, small epicontinental basins in an extensional geodynamic setting dominated by structural highs and subsident trenches, the latters filled with continental sediments mixed with minor magmatic-derived materials [8]. Therefore the Zn-Pb (-Ag) deposits testify to the occurrence of an important exhalative event of Upper Carboniferous age, previously unrecognized in the Ligurian Briançonnais Unit.

More work is needed in order to thoroughly characterize the anatomy of the hydrothermal system, even it is a difficult task in absence of drilling and/or underground data. Further studies in this and other areas of the Ligurian Briançonnais Unit, where also Zn-Pb (-Ag) occurrences *possibly* of the same origin occur, can help to better understand both the hydrothermal system(s) evolution and the Late Palaeozoic geodynamic and tectonic setting of this sector of the Alps, and to establish correlations between different tectonic units of the Briançonnais puzzle.

Acknowledgments

We are greatly indebted to C. Groppo for her help in the pseudosections calculations, and to D. Castelli and B. Lombardo for stimulating discussions; A. Marino’s help to find the first mineralizations in the bush was highly appreciated. The manuscript has been greatly improved by the comments and suggestions of two anonimous reviewers. This work was carried out with financial support of M.I.U.R., ex-60%. The MicroRaman data have been obtained with the equipment acquired by the Interdepartmental Center “G. Scansetti” for Studies on Asbestos and Other Toxic Particulates with a grant from Compagnia di San Paolo, Torino; minerals were analysed using the SEM-EDS microprobe installed at the Dipartimento di Scienze Mineralogiche e Petrologiche, Università di Torino.

References

[1] Franklin J.M., Sangster D.M., Lydon J.W., Volcanic-associated massive sulfide deposits, in: Skinner B.J. (Ed.), Economic Geology Seventy-fifth Anniversary Volume, Economic Geology Publishing Co., New Haven, 1981, pp. 485-627.

[2] Rona P.A., Hydrothermal mineralisation at seafloor spreading centers, Earth Sci. Rev. 20 (1984) 1-104.

[3] Goodfellow W.D., Zierenberg R.A., ODP Leg 169 Shipboard Science Party, Genesis of massive sulfide deposits at sediment-covered spreading centers, in: Barrie C.T., Hannington M.D. (Eds.), Volcanic-associated massive sulfide deposits: processes and examples in modern and ancient settings, Rev. Econ. Geology 8, Society of Economic Geology Inc., Boulder, 1999, pp. 297-324.

[4] Barrie C.T., Hannington M.D., Classification of volcanic-associated massive sulfide deposits based on host-rock composition, in: Barrie C.T., Hannington M.D. (Eds.), Volcanic-associated massive sulfide deposits: processes and examples in modern and ancient settings, Rev. Econ. Geology 8, Society of Economic Geology Inc., Boulder, 1999, pp. 1-12.

[5] Goodfellow W.D., Geology, genesis and exploration of SEDEX deposits, with emphasis on the Selwyn Basin, Canada, in: Deb M., Goodfellow W.D. (Eds.), Sediment-hosted Lead-Zinc Sulphide Deposits, Narosa Pub. House, New Delhi, 2004, pp. 24-99.

[6] Castelli D., Rostagno C., Lombardo B., Jd-Qtz-bearing metaplagiogranite from the Monviso meta-ophiolite (Western Alps), Ofioliti 27 (2002) 81-90.

[7] Mastrangelo F., Natale P., Zucchetti S., Quadro giacimentologico e metallogenico delle Alpi Occidentali italiane, Bollettino Associazione Mineraria Subalpina 20 (1983) 203-248.

[8] Vanossi M., Cortesogno L., Galbiati B., Messiga B., Piccardo G., Vannucci R., Geologia delle Alpi Liguri: dati, problemi, ipotesi, Mem. Soc. Geol. It. 28 (1984) 5–57.

[9] Seno S., Dallagiovanna G., Vanossi M., A kinematic evolutionary model for the Penninic sector of the central Ligurian Alps, Int. J. Earth Sci. 94 (2005) 114–129.

[10] Stampfli G.M., Le Briançonnais, terrain exotique dans les Alpes?, Eclogae Geol. Helv. 86 (1993) 1–45.

[11] Cortesogno L., Dallagiovanna G., Gaggero L., Vanossi M., Elements of the Palaeozoic history of the Ligurian Alps in: von Raumer J.F., Neubauer F. (Eds.), Pre-Mesozoic geology in the Alps, Springer, Berlin, 1993, pp. 257–278.

[12] Vanossi M. (Ed.), Guide geologiche regionali. Alpi Liguri, 2nd ed., BE-MA Rome, 1994, 293 p.

[13] Vanossi M., Perotti C.R., Seno S., The Maritime Alps arc in the Ligurian and Tyrrhenian systems, Tectonophysics 230 (1994) 75-89.

[14] Messiga B., Evidenze strutturali e paragenetiche dell'evoluzione polifasica pre-alpina del Massiccio Cristallino di Savona, Rend. Soc. It. Min. Petr. 37 (1981) 739–754.

[15] Cortesogno L., Metamorfismo e magmatismo prealpini nel basamento e nel tegumento delle Alpi liguri, Mem. Soc. Geol. It. 28 (1984) 79-95.

[16] Cortesogno L., Gianotti R., Oxilia M., Vanossi M., Vannucci R., Genesi ed evoluzione dello zoccolo pre-mesozoico di alcuni settori del Brianzonese ligure interno, Rend. Soc. It. Min. Petr. 38 (1982) 219-260.

[17] Messiga B., Il metamorfismo alpino nelle Alpi Liguri: alcuni aspetti petrologici, Mem. Soc. Geol. It. 28 (1984) 151–179.

[18] Cortesogno L., Dallagiovanna G., Vanossi M., Paléogéographie du Briançonnais ligure d'après les lithoclastes des formations permo-carbonifères, Géol. Alpine 14 (1988) 9-28.

[19] Cortesogno L., Dallagiovanna G., Gaggero L., Vanossi M., Late Variscan intermediate volcanism in the Ligurian Alps, Newsletter 5 (1992) 241-262.

[20] Cortesogno L., Gianotti R., Oddone M., Vannucci R., Vanossi M., Contributo alla conoscenza delle metavulcaniti tardo-erciniche del Brianzonese ligure (Alpi Marittime): i Porfidi di Osiglia e i clasti di vulcaniti nella Formazione di Ollano, Rend. Soc. It. Min. Petr. 39 (1984) 575-592.

[21] Cortesogno L., Gianotti R., Vannucci R., Vanossi M., Le volcanisme permo-carbonifère du Briançonnais ligure (Alpes Marittimes) dans

le cadre des phases tardives de l'orogenèse hercynienne, Bull. Sci. Géol. 37 (1984) 37-50.

[22] Messiga B., Oxilia M., Piccardo G., Vanossi M., Fasi metamorfiche e deformazioni alpine nel brianzonese e nel pre-piemontese esterno delle Alpi Liguri: un possibile modello evolutivo, Rend. Soc. It. Min. Petr. 38 (1981) 261–280.

[23] Cabella R., Cortesogno L., Dallagiovanna G., Vannucci R., Vanossi M., Vulcanismo, sedimentazione e tettonica nel Brianzonese ligure esterno durante il Permo-Carbonifero, Atti Ist. Geol. Univ. Pavia 31 (1988) 269-326.

[24] Cabella R., Cortesogno L., Dallagiovanna G., Gaggero L., Vanossi M., Nuovi dati sui terreni permo-carboniferi delle Alpi liguri centro-occidentali, Boll. Museo Reg. Sc. Nat. Torino 9 (1991) 119-139.

[25] Piccoli G.C., Minerali delle Alpi Marittime e Cozie. Provincia di Cuneo, L'Artistica Savigliano, 2002, 366 p.

[26] Barelli V., Cenni di statistica mineralogica degli Stati di S.M. il Re di Sardegna, ovvero Catalogo ragionato della raccolta formatasi presso l'Azienda Generale dell'Interno, Fodratti, Torino, 1835, 686 p.

[27] Casalis G., Dizionario geografico storico-statistico-commerciale degli Stati di S. M. il re di Sardegna, Maspero, Torino, 1840, 870 p.

[28] Jervis G., I tesori sotterranei dell'Italia. Parte prima: Regione delle Alpi, Loescher, Torino, 1873, 410 p.

[29] Ferrero S., Le mineralizzazioni a solfuri massivi di Casario (Priola, Alpi Liguri): studio geologico e petrografico, M. Sci. Thesis, University of Turin, 2006, 159 p.

[30] Downs R.T., The RRUFF Project: an integrated study of the chemistry, crystallography, Raman and infrared spectroscopy of minerals, Program and Abstracts 19th General Meeting IMA, Kobe, Japan, 2006, O03-13.

[31] Lucchetti G., Cabella R., Cortesogno L., Pumpellyites and coexisting minerals in different low-grade metamorphic facies of Liguria, Italy, J. Metam. Geol. 8 (1990) 539–550.

[32] Goffé B., Le faciès à carpholite-chloritoide dans la couverture briançonnaise des Alpes Ligures: un témoin de l'histoire tectonométamorphique régionale, Mem. Soc. Geol. It. 28 (1984) 461-479.

[33] Vidal O., Goggé B., Theye T., Experimental study of the stability of sudoite and magnesio-carpholite and calculation of a petrogenetic grid for the system FeO-MgO-Al_2O_3-SiO_2-H_2O, J. Metam. Geol. 10 (1992) 603-614.

[34] Goffé B., Schwartz S., Lardeaux J.M., Bousquet R., Explanatory notes to the map: Metamorphic structure of the Alps – Western and Ligurian Alps, Mitt. Österr. Miner. Ges. 149 (2004) 124-144.

[35] Groppo C., Castelli D., Compagnoni R., Late chloritoid-staurolite assemblage in a garnet-kyanite-bearing metapelite from the ultrahigh-pressure Brossasco-Isasca unit (Dora-Maira Massif, Western Alps): new petrological constraints for a portion of the decompressional path, in: Hacker B.R., McClelland W.C., Liou J.G. (Eds.), Ultrahigh-pressure metamorphism: deep continental subduction, Geological Society of America, Boulder, 2006, pp. 127-138.

[36] Connolly J.A.D., Multivariable phase diagrams: an algorithm based on generalized thermodynamics, Am. J. Sci. 290 (1990) 666-718.

[37] Holland T.J.B., Powell R., An internally consistent thermodynamic data set for phases of petrologic interest, J. Metam. Geol. 16 (1988) 309-343.

[38] Bucher K., Frey M., Petrogenesis of metamorphic rocks, 7th ed., Springer, Berlin, 2002, 341 p.

[39] Messiga B., Alpine metamorphic evolution of Ligurian Alps (North-West Italy): chemography and petrological constraints inferred from metamorphic climax assemblages, Contrib. Mineral. Petrol. 95 (1987) 269-277.

[40] Large R., McGoldrick P., Bull S., Cooke D., Proterozoic stratiform sediment-hosted zinc-lead-silver deposits of Northern Australia, in: Deb M., Goodfellow W.D. (Eds.), Sediment-hosted Lead-Zinc Sulphide Deposits, Narosa Pub. House, New Delhi, 2004, pp. 1-23.

[41] Lydon J.W., Volcanogenic massive sulphide deposits, part I: a descriptive model, Geosciences Canada 11 (1984) 195–202.

[42] Lydon J.W., Volcanogenic massive sulphide deposits, part II: genetic models, Geosciences Canada 15 (1988) 43–65.

[43] Goodfellow W.D., Lydon J.W., Turner L.J.W, Geology and genesis of stratiform sediment-hosted (SEDEX) zinc-lead-silver sulphide deposits, Geol. Assoc. Canada Spec. Paper 40 (1993) 201-252.

[44] Large R.R., Bull S.W., Cooke D.R., McGoldrick P.J., A genetic model for the HYC deposit, Australia, based on regional sedimentology, geochemistry, and sulfide-sediments relationships, Econ. Geol. 93 (1998) 1345-1368.

[45] Cook N.J., Chryssoulis S.L., Concentrations of ‘‘invisible’’ gold in the common sulfides. Canadian Mineralogist 28 (1990) 1–16.

[46] Johan Z., Marcoux E., Bonnemaison M., Arsénopyrite aurifère: mode de substitution de Au dans la structure de FeAsS, Comptes Rendus Acad. Sciences Paris 308 (1989) 185-191.

[47] Zacharias J., Fryda J., Paterova B., Mihaljevic M., Arsenopyrite and As-bearing pyrite from the Roudny deposit, Bohemian Massif, Mineral. Magazine 68 (2004) 31-46.

[48] Craig J.R., Vokes F.M., Solberg T.N., Pyrite: physical and chemical textures, Mineralium Deposita 34 (1998) 82-101.

[49] Ramdohr P., Mineralbestand, Strukturen und Genese der Rammelsberg Lagerstätte, Geol. Jahrb. 67 (1953) 367-494.

[50] Ramdohr P., The ore minerals and their intergrowths, Pergamon Press, Oxford, 1980, 1207 p.

[51] Hannington M.D., Galley A.G., Herzig P.M., Petersen S., Comparison of the TAG mound and stockwork complex with Cyprus-type, massive sulfide deposits, in: Herzig P.M., Humphris S.E., Miller D.J., Zierenberg R.A. (Eds.), Proceedings of the ODP, Scientific results 158, 1988, pp. 389-416.

[52] Sarkar S.C., Banerjee S., Carbonate-hosted lead-zinc deposits of Zawar, Rajasthan, in the context of the world scenario, in: Deb M., Goodfellow W.D. (Eds.), Sediment-hosted Lead-Zinc Sulphide Deposits, Narosa Pub. House, New Delhi, 2004, pp. 328-349.

[53] Stanton R.L., On limits to distances of movement of matter during regional metamorphism: an investigation of nine samples from high-grade metamorphic terranes, Canadian Mineralogist 44 (2006) 985-1024.

[54] Chauhan D.S., Sedimentary pyrite from Pb-Zn deposits of the Zawar and Rajpura – Dariba regions and its bearing on the genesis of base metal sulfides, in: Wauschkuhn A., Luth C., Zimmermann R.A. (Eds.), Syngenesis and epigenesis in the formation of mineral deposits, Springer-Verlag, Berlin, 1984, pp. 36-42.

[55] Large D.E., Geological parameters associated with sediment-hosted, submarine exhalative Pb-Zn deposits: an empirical model for mineral exploration, Geologisches Jahrbuch 40 (1980) 59-129.

[56] Large D.E., Sediment-hosted submarine exhalative lead-zinc deposits – a review of their geological characteristics and genesis, in: Wolf K.H. (Ed.), Handbook of strata-bound and stratiform ore deposits, vol. 9, Elsevier, Amsterdam, 1981, pp. 469-507.

[57] Carne R.C., Cathro R.J., Sedimentary exhalative (sedex) zinc-lead-silver deposits, northern Canadian Cordillera, Can. Inst. Mining Bull. 76 (1982) 66-78.

[58] Stanton R.L., Gorman H., A phenomenological study of grain boundary migration in some common sulfides, Econ. Geol. 63 (1968) 907-923.

[59] Lusk J., Calder B.O.E., Freeman T. E., Temperatures from triple-junction angles in sulfides, American Mineralogist 87 (2002) 1390–1400.

[60] Barton P.B., Skinner B.J., Sulfide mineral stabilities, in: Barnes H.L. (Ed.), Geochemistry of Hydrothermal Ore Deposits, IInd ed., John Wiley & Sons, New York, 1979, pp. 278–403.